Supporting Information

to

Access to Pure and Highly Volatile Hydrochalcogenide Ionic Liquids

*L. H. Finger,[a] F. Wohde,[a] E. I. Grigoryev,[a] A.-K. Hansmann,[a] R. Berger,[a] B. Roling[a] and J. Sundermeyer[a]**

a) Fachbereich Chemie,
Philipps-Universität Marburg,
Hans-Meerwein-Str. 4,
35043 Marburg,
Germany.
*E-Mail: JSU@staff.uni-marburg.de

Content

1. Devices and methods

Elemental analyses (C, N, H, S) were carried out by the service department for routine analysis and mass spectrometry with a vario MICRO cube (ELEMENTAR). The samples were weighed into tin capsules inside a nitrogen filled glove box (Labmaster 130, MBRAUN).

Melting points were determined with a BÜCHI Melting Point B540.

Combined TGA/ DSC measurements were performed with a NETZSCH STA 409 CD in aluminium oxide crucibles, with an argon flow rate of 40 mL/min and a heating rate of 10 K/min; TGA decomposition points are given as onset temperature, DSC data is given as peak value.

^{1}H and ^{13}C-NMR spectra were recorded in automation with a BRUKER Avance 300 spectrometer, ^{77}Se NMR-spectra were recorded by the service department for NMR-analyses with a BRUKER DRX 400 spectrometer. All spectra were recorded at ambient temperature. ^{1}H and ^{13}C-NMR spectra were calibrated using residual protons and solvent signals, respectively (DMSO-d_6: δ_H 2.50 ppm, δ_C 39.52 ppm).[1] NMR spectra of ^{77}Se were referenced externally against dimethyl selenide.

IR spectra were recorded on a BRUKER APLPHA FT-IR spectrometer with Platinum ATR-sampling.

2. Starting materials

All solvents were dried according to common procedures[2] and passed through columns of aluminium oxide, 3 Å molecular sieve and R3-11G-catalyst (BASF) or stored over molecular sieve (3 or 4 Å) until use. Reagents were used as received unless stated otherwise. 1-Ethyl-3-methylimidazolium methylcarbonate in methanol solution (30%) was donated by BASF. 1-Butyl-3-methylimidazolium methylcarbonate in methanol solution (50%) was purchased from IOLITEC, *N*-butylpyrrolidine from ACROS. 1-Ethyl-2-methylimidazole was synthesised in analogy to a published procedure.[3] Methylcarbonate ionic liquids were synthesised following the general procedure of R. Kalb.[4] Bis(trimethylsilyl) selenide was synthesised in analogy to the corresponding sulphide.[5]

3. Synthetic Procedures

3.1 Synthesis of 1-ethyl-3-methylimidazolium hydrosulphide ([EMIm][HS], 1).

Hydrogen sulphide was fed into a 30% solution of 1-ethyl-3-methylimidazolium methylcarbonate (26.9 g, 43.4 mmol) in methanol for 40 minutes. All volatiles were removed *in vacuo* and the residue recrystallised from a mixture of acetonitrile and diethyl ether at −30 °C. The solution was decanted and the crystals dried in fine vacuum. [EMIm][HS] (4.62 g, 32.0 mmol, 74%) was obtained as colourless solid. **Mp** 91-93 °C (from acetonitrile/ diethyl ether, 2 K/min). **DSC** (10 K/min): 92.8 °C (endoth.). **TGA** (10 K/min): 162.1 °C (decomp.). **Elem. anal.** found C, 49.9; H, 8.6; N, 19.6; S, 22.0; $C_6H_{12}N_2S_1$ requires C, 50.0; H, 8.4; N, 19.4; S, 22.2. **IR:** ν_{max}/cm^{-1}: 3022m, 2859m, 2565w (SH), 1570s, 1464m, 1420m, 1339m, 1178s, 1030w, 874m, 800s, 704w, 622vs. **^{1}H-NMR** (300.1 MHz, DMSO-d_6) $\delta_H = -3.85$ (s, 1H, *H*S), 1.39 (t, $^3J_{HH}$ = 7.3 Hz, 3H, CH_2CH_3), 3.88 (s, 3H, N*Me*), 4.24 (q, $^3J_{HH}$ = 7.3 Hz, 2H, CH_2CH_3), 7.87 (s, 1H, *H*4/5), 7.99 (s, 1H, *H*4/5), 9.97 (s, 1H, *H*2) ppm. **^{13}C-NMR** (75.5 MHz, DMSO-d_6): $\delta_C = 15.2$ (1C, CH_2CH_3), 35.6 (1C, N*Me*), 43.9 (1C, CH_2CH_3), 121.9 (1C, *C4/5*), 123.3 (1C, *C4/5*), 136.7 (1C, *C2*) ppm.

For sublimation [EMIm][HS] (535 mg, 3.71 mmol) was placed in a long Schlenk tube and heated to 70 °C at $1 \cdot 10^{-3}$ mbar. A colourless substance sublimed to the cooler parts of the flask. After 18 hours 465 mg (3.22 mmol, 87%) of purified, colourless [EMIm][HS] could be isolated. The light brown remainder (30 mg) consisted primarily of unchanged starting material. **Mp:** 92-93 °C**. Elem. anal.** found C, 50.0; H, 8.4; N, 19.7; S, 22.1; $C_6H_{12}N_2S_1$ requires C, 50.0; H, 8.4; N, 19.4; S, 22.2. The IR and NMR spectra stayed unchanged.

3.2 Synthesis of 1-ethyl-2,3-dimethylimidazolium hydrosulphide ([EMMIm][HS], 2).

1-Ethyl-2,3-dimethylimidazolium methylcarbonate (12.7 g, 63.4 mmol) was dissolved in methanol (20 mL) and hydrogen sulphide was fed into the solution for 75 minutes. All volatile components were removed in vacuum, and the residue recrystallised from a mixture of acetonitrile and diethyl ether. [EMMIm][HS] was isolated as light orange crystals in a yield of 4.60 g (29.1 mmol, 46%). **Mp** 125-126 °C (from acetonitrile/ diethyl ether, 2 K/min). **DSC** (10 K/min): 127.6 °C (endoth.). **TGA** (10 K/min): 179.5 °C (decomp.). **Elem. anal.** found C, 53.1; H, 9.1; N, 18.0; S, 19.0; $C_7H_{14}N_2S_1$ requires C, 53.1; H, 8.9; N, 17.7; S, 20.3. **IR:**

ν_{max}/cm^{-1}: 2971s, 2563m (HS), 1721w, 1580m, 1533m, 1327w, 1299m, 1253s, 1197m, 1128m, 954w, 818vs, 661m, 500w. **^{1}H-NMR** (300.1 MHz, DMSO-d_6) δ_H = −4.07 (s, 1H, *H*S), 1.33 (t, $^{3}J_{HH}$ = 7.3 Hz, 3H, CH_2CH_3), 2.60 (s, 3H, C-*Me*), 3.76 (s, 3H, N*Me*), 4.16 (q, $^{3}J_{HH}$ = 7.3 Hz, 2H, CH_2CH_3), 7.69 (s, 1H, *H*4/5), 7.73 (s, 1H, *H*4/5). **^{13}C-NMR** (75.5 MHz, DMSO-d_6): δ_C = 9.0 (1C, C-*Me*), 14.8 (1C, CH_2CH_3), 34.6 (1C, N*Me*), 42.7 (1C, CH_2CH_3), 120.3 (1C, *C4/5*), 122.3 (1C, *C4/5*), 144.0 (1C, *C2*) ppm.

For sublimation [EMMIm][HS] (349 mg, 2.21 mmol) was placed in a long Schlenk tube and heated to 85 °C at $1 \cdot 10^{-3}$ mbar. A colourless substance sublimed to the cooler parts of the flask. After 60 hours 284 mg (1.79 mmol, 81%) of purified, colourless [EMMIm][HS] could be isolated. The red remainder consisted partly of [EMMIm][HS] but mostly unidentifiable side and decomposition products. **Mp** 127-128 °C. **Elem. anal.** found C, 53.1; H, 9.1; N, 18.1; S, 20.4; $C_7H_{14}N_2S_1$ requires C, 53.1; H, 8.9; N, 17.7; S, 20.3. The IR and NMR spectra stayed unchanged.

3.3 Synthesis of 1-butyl-3-methylimidazolium hydrosulphide ([BMIm][HS], 3).

A 50% solution of 1-butyl-3-methylimidazolium methylcarbonate (8.39 g, 39.1 mmol) in methanol was mixed with additional methanol (10 mL) and hydrogen sulphide was fed into the solution for 45 minutes. All volatiles were removed *in vacuo* and the residue recrystallised from a mixture of acetonitrile and diethyl ether at −30 °C. The solution was decanted and the crystals dried in fine vacuum. [BMIm][HS] (3.54 g, 53%) was obtained as colourless solid. **Mp** 54-55 °C (from acetonitrile/ diethyl ether, 2 K/min). **DSC** (10 K/min): 56.0 °C (endoth.). **TGA** (10 K/min): 157.4 °C (decomp.). **Elem. anal.** found C, 55.8; H, 9.6; N, 16.7; S, 18.55; $C_8H_{16}N_2S_1$ requires C, 55.8; H, 9.4; N, 16.3; S, 18.6. **IR:** ν_{max}/cm^{-1}: 2928m, 2806m, 2559w (HS), 1665w, 1556s, 1453m, 1418w, 1362w, 1165vs, 1011m, 908m, 801s, 753m, 655s, 630s. **^{1}H-NMR** (300.1 MHz, DMSO-d_6) δ_H = −3.92 (s, 1H, *H*S), 0.88 (t, $^{3}J_{HH}$ = 7.3 Hz, 3H, CH_2CH_3), 1.18-1.30 (m, 2H, CH_2CH_3), 1.71-1.81 (m, 2H, NCH_2CH_2), 3.88 (s, 3H, N*Me*), 4.20 (t, $^{3}J_{HH}$ = 7.2 Hz, 2H, NCH_2CH_2), 7.81 (s, 1H, *H*4/5), 7.90 (s, 1H, *H*4/5), 9.76 (s, 1H, *H*2) ppm. **^{13}C-NMR** (75.5 MHz, DMSO-d_6) δ_C = 13.2 (1C, CH_2CH_3), 18.7 (1C, CH_2CH_3), 31.3 (1C, NCH_2CH_2), 35.6 (1C, N*Me*), 48.3 (1C, NCH_2CH_2), 121.1 (1C, *C4/5*), 123.4 (1C, *C4/5*), 136.7 (1C, *C2*) ppm.

For sublimation [BMIm][HS] (549 mg, 3.19 mmol) was placed in a long Schlenk tube and heated to 50 °C at $1 \cdot 10^{-3}$ mbar. A colourless substance sublimed to the cooler parts of the flask. After 48 hours 420 mg (1.79 mmol, 77%) of purified, colourless [BMIm][HS] could be

isolated. The light green remainder consisted of unchanged starting material. **Mp** 54-55 °C. **Elem. anal.** found C, 55.8; H, 9.5; N, 16.7; S, 18.3; $C_8H_{16}N_2S_1$ requires C, 55.8; H, 9.4; N, 16.3; S, 18.6. The IR and NMR spectra stayed unchanged.

3.4 Synthesis of 1-ethyl-3-methylimidazolium hydroselenide ([EMIm][HSe], 4).

A 30% solution of 1-ethyl-3-methylimidazolium methylcarbonate (3.68 g, 5.93 mmol) was cooled in an ice bath and degassed thoroughly. Bis(trimethylsilyl)selenide (1.63 g, 7.23 mmol) was added in small portions within 15 minutes and the resulting mixture was stirred at 0 °C for 30 minutes and further 30 minutes at ambient temperature. After removal of volatile contents the residue was recrystallised from an acetonitrile/ diethylether mixture at −30 °C. [EMIm][HSe] (796 mg, 70%) was obtained as a colourless solid. **Mp** 101-102 °C (from acetonitrile/ diethyl ether, 2 K/min). **Elem. anal.** found C, 37.7; H, 6.4; N, 15.0; $C_6H_{12}N_2Se_1$ requires C, 37.7; H, 6.3; N, 14.7. **IR:** ν_{max}/cm^{-1}: 3049m, 2962m, 2274w (HSe), 1569m, 1418w, 1362w, 1339w, 1259m, 1173s, 1091m, 1027m, 863m, 789vs, 704m, 645m, 620vs. **^{1}H-NMR** (300.1 MHz, DMSO-d_6) $\delta_H = -6.56$ (s, 1H, *H*Se), 1.40 (t, $^3J_{HH} = 7.3$ Hz, 3H, CH_2CH_3), 3.87 (s, 3H, N*Me*), 4.22 (q, $^3J_{HH} = 7.3$ Hz , 2H, CH_2CH_3), 7.77 (t, $^{3/4}J_{HH} = 1.7$ Hz, 1H, *H4/5*), 7.87 (t, $^{3/4}J_{HH} = 1.7$ Hz, 1H, *H4/5*), 9.46 (s, 1H, *H2*) ppm. **^{13}C-NMR** (75.5 MHz, DMSO-d_6): $\delta_C = 15.1$ (1C, CH_2CH_3), 35.7 (1C, N*Me*), 44.0 (1C, CH_2CH_3), 121.9 (1C, *C4/5*), 123.4 (1C, *C4/5*), 136.2 (1C, *C2*) ppm. **^{77}Se-NMR** (76.3 MHz, DMSO-d_6): $\delta_{Se} = -312.3$ ppm.

For sublimation [EMIm][HSe] (418 mg, 2.19 mmol) was placed in a long Schlenk tube and heated to 95 °C at $1 \cdot 10^{-3}$ mbar. A colourless substance sublimed to the cooler parts of the flask. After 80 hours 330 mg (1.73 mmol, 79%) of purified, colourless [EMIm][HSe] could be isolated. The light green remainder consisted of unchanged starting material. **Mp** 101-103 °C. **Elem. anal.** found C, 37.6; H, 6.3; N, 15.2.; $C_6H_{12}N_2Se_1$ requires C, 37.7; H, 6.3; N, 14.7. The IR and NMR spectra stayed unchanged.

3.5 Synthesis of N-butyl-N-methylpyrrolidinium hydrosulphide ([BMPyr][HS], 5).

N-Butyl-*N*-methylpyrrolidinium methylcarbonate (15.1 g 69.5 mmol) was dissolved in methanol (40 mL) and hydrogen sulphide fed into the solution for one hour. All volatiles were removed *in vacuo* and the residue recrystallised from a mixture of acetonitrile and diethyl ether at −30 °C. The solution was decanted and the crystals dried in fine

vacuum. [BMPyr][HS] (5.65 g, 46%) was obtained as colourless solid. **Mp** 153-155 °C (decomp., from acetonitrile/ diethyl ether, 2 K/min). **DSC** (10 K/min): 166.5 °C (endoth.). **TGA** (10 K/min): 153.4 °C (decomp.). **Elem. anal.** found C, 61.8; H, 12.3; N, 8.1; S, 17.7; $C_9H_{21}N_1S_1$ requires C, 61.65; H, 12.1; N, 8.0; S, 18.3. **UV-Vis**: λ_{max} (DMSO)/nm 264. **IR:** ν_{max}/cm^{-1}: 2959vs, 2934s, 2873m, 2560w (HS), 1459vs, 1379w, 1260w, 1060m, 1004s, 910s, 743m, 587w. **^{1}H-NMR** (300.1 MHz, DMSO-d_6) $\delta_H = -4.03$ (s, 1H, *H*S), 0.92 (t, $^3J_{HH} = 7.4$ Hz, 3H, CH_2CH_3), 1.24-1.38 (m, 2H, CH_2CH_3), 1.60-1.74 (m, 2H, NCH_2CH_2), 2.00-2.14 (m, 4H, *CH_2(3,4)*), 3.02 (s, 3H, N*Me*), 3.30-3.60 (m, 6H, NCH_2CH_2, *CH_2(2,5)*) ppm. **^{13}C-NMR** (75.5 MHz, DMSO-d_6) $\delta_C = 13.4$ (1C, CH_2CH_3), 19.2 (1C), 21.0 (1C), 24.8 (1C), 47.4 (t, $^3J_{CN} = 3.9$ Hz, 2C, *C3/4*), 62.6 (t, $^2J_{CN} = 2.8$ Hz, 2C, *C2/5*), 63.2 (t, $^2J_{CN} = 3.1$ Hz, 1C) ppm.

Upon attempting to sublime the substance analogously to the prior imidazolium salts the condensation of colourless droplets at cooler parts of the Schlenk flask was observed. These were identified as a mixture of decomposition products. No traces of the former salt could be detected.

4. Crystal Structures

Single crystals of [EMIm][HS] (**1**), where grown by sublimation, the resulting structure was analogous but of higher quality when compared to crystals grown from a saturated methanol solution. Crystals of **2** were obtained by layering a solution of the compound in acetonitrile with diethyl ether. [BMPyr][HS] (**5**) crystallised from an oversaturated acetonitrile solution at room temperature. The data collection for the single crystal structure determinations was performed in rotation method on a Bruker D8 QUEST diffractometer by the X-ray service department of the Fachbereich Chemie, University of Marburg. The spectrometer is equipped with a Mo-K_α X-ray micro source (0.71073 Å, Incotec), a fixed chi goniometer and a PHOTON 100 CMOS detector. Bruker software (Bruker Instrument Service, APEX2, SAINT) was used for data collection, cell refinement and data reduction.[6] The structures were solved with SIR-97[7] or SIR2011[8] refined with SHELXL-2014[9] and finally validated using PLATON[10] software, all within the WinGX[11] software bundle. EnCIFer aided in the editing and validation of the CIF files.[12] Absorption corrections where applied beforehand within the APEX2 software (multi-scan).[13] Graphic representations were created using Diamond 4.[14] C-bound H-atoms were constrained to parent site; The sulphur bound H-atom in [EMIm][HS] was located in the Fourier map and refined independently. Analogous treatment of the sulphur bound H-atom in [BMPyr][HS], did not lead to a stable position for the H-atom and convergence of the structure, possibly attributable to the strong disorder of the cation along a mirror plane (figure S1 and S2). In this case the H-atom was located in the Fourier map and coordinates and displacement were fixed before the next refinement cycles. In all graphics the ellipsoids are shown for the 50% probability level. Hydrogen atoms are shown with arbitrary radius, only those bound to hetero atoms or involved in hydrogen bonds are shown in the graphic representations. Selected crystal data and experimental parameters are listed in table S1. Crystallographic data for the structures presented in this paper have been deposited with the Cambridge Crystallographic Data Centre. CCDC-141450 and 141454 contain the supplementary crystallographic data for this paper. These data can be obtained free of charge from The Cambridge Crystallographic Data Centre via www.ccdc.cam.ac.uk/data%5Frequest/cif.

Table S1. Crystal data for the structures of compounds 1 and 5.

	[EMIm][HS] (**1**)	[BMPyr][HS] (**5**)
Formula	C6 H12 N2 S	C9 H21 N S
FW / g mol^{-1}	144.24	175.33
Crystal system	monoclinic	tetragonal
Space group	P 21/n	P 42/m b c
Colour, habit	colourless block	colourless needle
Crystal size / mm^3	0.21 x 0.20 x 0.10	0.38 x 0.14 x 0.12
a / Å	8.6023(3)	15.6635(6)
b / Å	7.6710(2)	15.6635
c / Å	12.7600(4)	8.9408(5)
α /°	90	90
β /°	107.8620(10)	90
γ /°	90	90
V / Å^3	801.42(4)	2193.6(2)
Z	4	8
D_{calc}/g cm^{-3}	1.195	1.062
Min./max. Transm.	0.6361/ 0.7457	0.6668/ 0.7456
μ / cm^{-1}	0.323	0.244
F(000)	312	784
T / K	100(2)	100(2)
θ range /°	2.54 : 26.33	2.60 : 25.99
range h,k,l	−11:11; −10:10; −17:17	−16:19; −18:19; −11:11
Refl. Coll.	18404	16725
Refl. Indep.	1993	1154
Refl. I > 2σ(I)	1777	871
Data / restr. / param.	1993/ 0/ 88	1154/ 2/ 90
R_{int}	0.0447	0.0514
R_1 (obs)	0.0318	0.0601
wR_2 (all)	0.0876	0.1680
GooF (F^2)	1.066	1.056
Res. e$^-$ dens. (min./ max.)	−0.238/ 0.338	−0.368/ 0.248
CCDC	1414150	1414154

Table S2. Hydrogen bonds in the solid state structure of [EMIm][HS] (1).

D-H···A	d(H···A) /Å	d(D···A) /Å	<(DHA)/°
[EMIm][HS], (**1**)			
C2-H2…S1’	2.68	3.520(1)	148.2
C4-H4…S1’’	2.79	3.731(1)	172.7
C6-H6B…S1	2.88	3.786(1)	152.7
I: x+1/2, −y+3/2, z−1/2; II: −x+1, −y+1, −z+1.			

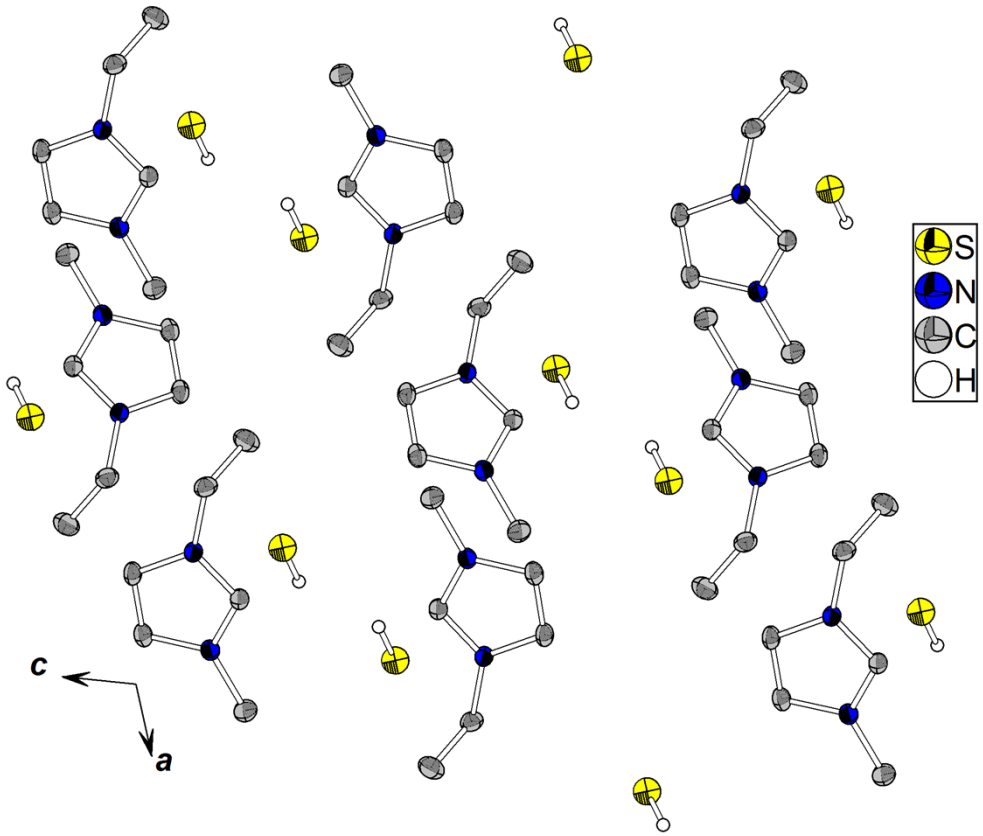

Figure S1. Crystal structure of [EMIm][HS] (1) viewing along the b-axis.

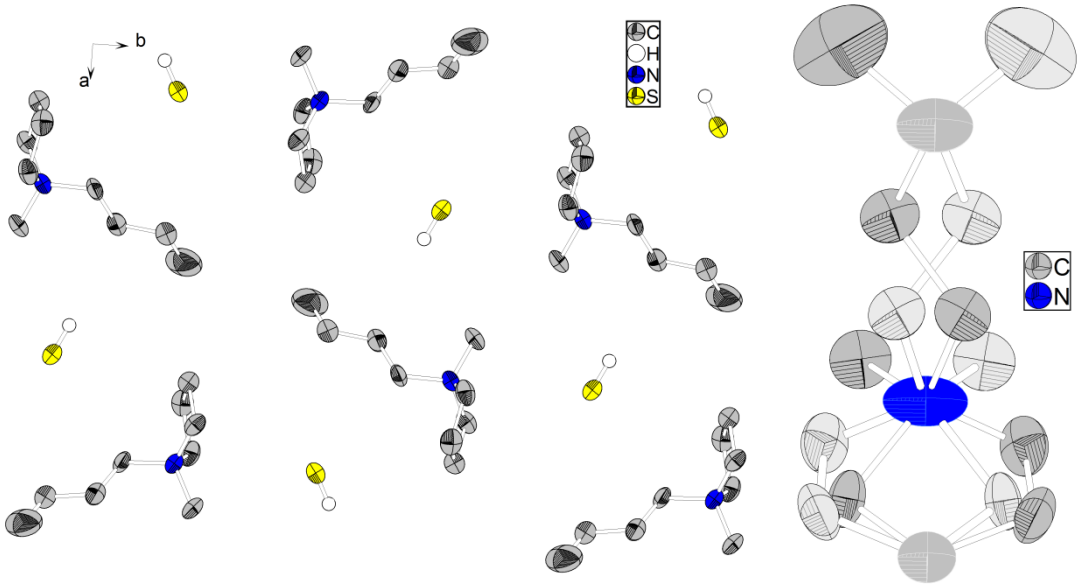

Figure S2. Crystal structure of [BMPyr][HS] (5) viewing along the c-axis and disorder of the pyrrolidinium cation along a mirror plane.

5. Details concerning the sublimation process

All sublimed imidazolium salts could unambiguously be identified as the original hydrochalcogenide salt. The NMR and IR spectra fully coincide; the elemental composition was proven by elemental analysis (CHNS). The melting points were increased by ca. 1 K after sublimation demonstrating the already high purity of the originally isolated hydrochalcogenide salts. The residue after a first sublimation consists mainly of unsublimed starting material, only in case of [EMMIm][HS] (**2**) a larger amount of unidentified side products was observed. Typically the isolated sublimate accounted for more than 80% of the employed amount. After a second sublimation no visible residue remained, 95% of the deployed substance could be re-isolated.

Figure S3. Crystals of [EMIm][HS] (1) after sublimation.

Figure S4. [EMMIm][HS] (2) before and after sublimation.

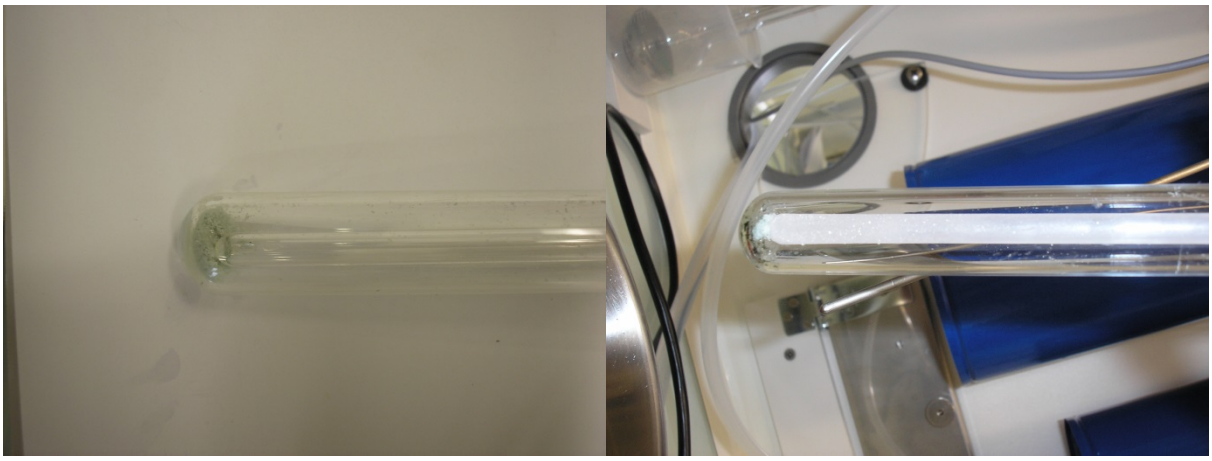

Figure S5. [BMIm][HS] (2) before and after sublimation.

Figure S6. Crystalline [BMIm][HS] (3) after sublimation.

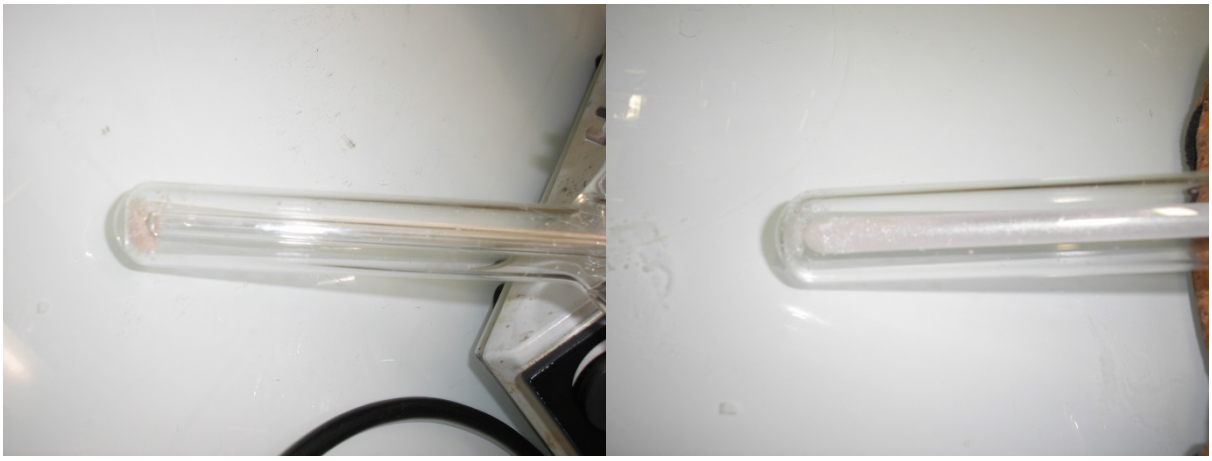

Figure S7. [EMIm][HSe] (4) before and after sublimation.

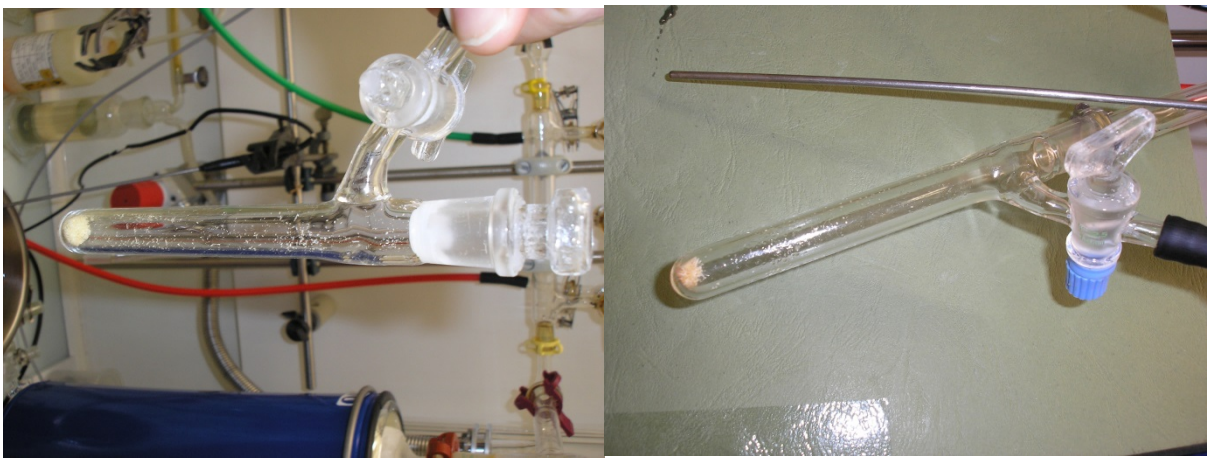

Figure S8. [BMPyr][HS] (5) before and after the attempted sublimation, the right picture shows the oily decomposition products.

In case of [BMPyr][HS] the condensated substance consists primarily of the acyclic aminothiole S**7**, which results from a ring opening S_N2 attack at one of the pyrrolidinium C atoms next to the nitrogen atom. This reaction behaviour is well documented for pyrrolidinium cations. It can be traced back to an increased ring strain in comparison with related 6-ring piperidinium, where primarily a demethylation occurs.[15]

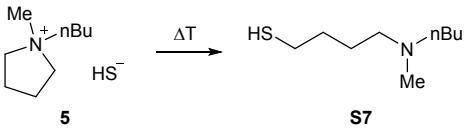

5 **S7**

Scheme S1. Thermal decomposition of [BMPyr][HS] (5), only the main product is shown.

We also investigated the vaporisation behaviour of the hydrosulphide salts **1** and **5** under ambient pressure, in order to mimic the conditions in the TGA measurements for ΔH_{vap} determination (*vide infra*). Larger samples were placed in a Schlenk tube with a coldfinger at −30 °C reaching as far as 1 cm above the substance. The tube was then heated to 100 °C and after reaching the final temperature the pressure was adjusted to atmospheric conditions. After several hours, when a sufficient amount of material was visible on the cold finger, the experiment was stopped and the complete condensate analysed by NMR spectroscopy. Figures S9 compares the ^{1}H-NMR spectra of pure [EMIm][HS] and the collected substance, figure S10 correspondingly compares the spectra of [BMPyr][HS] and its decomposition products.

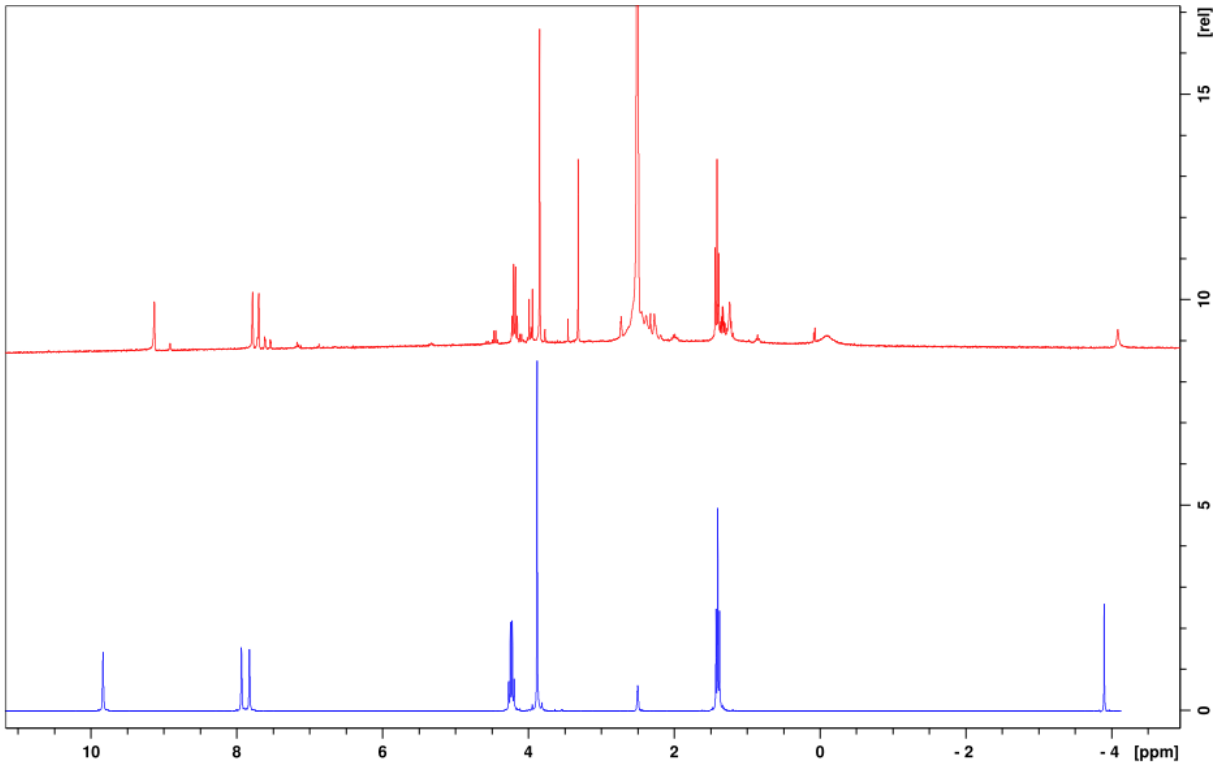

Figure S9. ^{1}H-NMR spectra of pure [EMIm][HS] (blue) and the substance collected after the attempted sublimation at ambient pressure (red). The variation of the chemical shift of the aromatic imidazolium protons is due to the difference in concentration of the two samples.

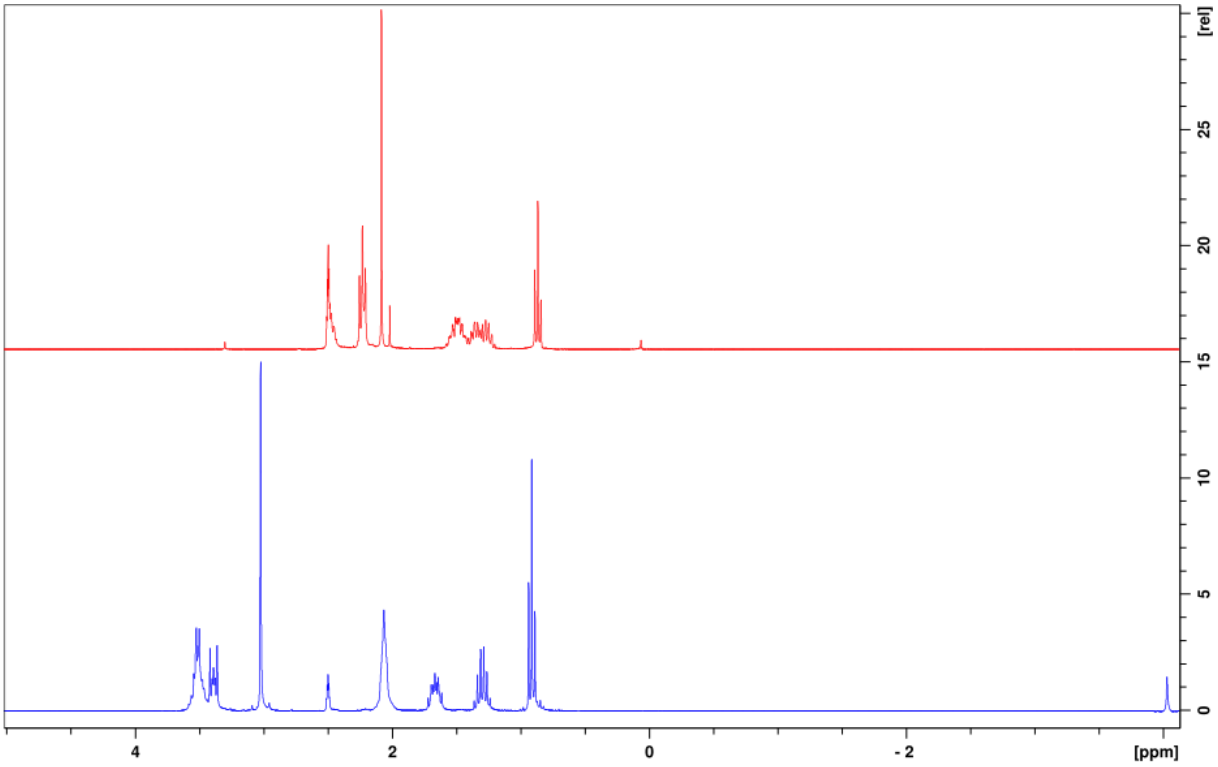

Figure S10. 1H-NMR spectra of pure [BMPyr][HS] (blue) and the decomposition products collected after the attempted sublimation at ambient pressure (red).

6. Isothermal TGA measurements for ΔH_{vap} determination

Isothermal TGA experiments for determination of vaporisation enthalpies were conducted using a TGA/SDTA 851 equipped with a LF/1100 °C oven from METTLER TOLEDO. The measurements were carried out in encapsulated 40 µL Al crucibles, which have been perforated with a 0.64 mm opening for a defined effusion at isothermal steps. Dry nitrogen was used as carrier gas with a flow rate of 50 mL/min. The calibration of the experimental setup was undertaken with ferrocene as calibration substance with known vapour pressure, following the NIST recommendation.[16] Ferrocene was purchased from ACROS ORGANICS (98%)

For all experiments the purest available samples were chosen; in case of the imidazolium salts, the salts were sublimed once before further use. In case of [BMPyr][HS] a double recrystallisation of the sample was carried out. As further test substance for the TGA experiments, [BMIm][TFSI] was purchased from IOLITEC (99.5%) and dried 24 h in fine vacuum at 90 °C prior to the TGA experiment. All measurements were conducted with a stepwise temperature programme of isothermal plateaus (10 min) and a heating rate of 10 K/min. The mass loss rate per unit area $\frac{1}{A} \cdot \left|\frac{dm}{dt}\right|_T$ is related to the apparent vapour pressure P_T via equation (1):[16a]

$$log\left(\frac{1}{A} \cdot \left|\frac{dm}{dt}\right|\right)_T + C \propto log\ P_T \qquad (1)$$

Here, C is a device specific constant.

From Arrhenius plots of the mass loss rates per unit area, the vaporisation enthalpy ΔH_{vap} could be extracted according to the Clausius-Clapeyron equation (2), where C' is a sample specific constant.

$$\log\left(\frac{1}{A} \cdot \left|\frac{dm}{dt}\right|\right) = \frac{\Delta H_{vap}}{R} \cdot \frac{1000}{T} + C' \qquad (2)$$

The determined ΔH_{vap} values were corrected to 298 K via equation (3).

$$\Delta H_{vap}(298\ K) = \Delta H_{vap}\,(T_{av}) + \Delta C_m(298\ K - T_{av}) \qquad (3)$$

The value of the molar heat capacity difference ΔC_m was set to -0.1 kJ•mol^{-1}, which has evolved as a rough standard approximation in this field of research, although not undisputed.[17]

To allow for a comparison of the apparent vapour pressures between different substances, the molar weight of the gas-phase molecules has to be considered. Here, we assumed contact ion pairs to constitute the gas phase. Therefore, the IL-specific molar masses were employed to the Arrhenius plots of the molar loss rates per unit area $log\left(\frac{1}{A}\cdot\left|\frac{dn}{dt}\right|\right) = log\left(\frac{1}{A}\cdot\left|\frac{dm}{dt}\right|\cdot\frac{1}{M}\right)$, presented in figure S11-right, compared with the mass loss rate (figure S11-left). Comparing substances **1**, **2**, **5**, ferrocene and [BMIm][TFSI] shows the striking difference between the classical IL test substance [BMIm][TFSI] and the hydrochalcogenides investigated in this work (figure S12).

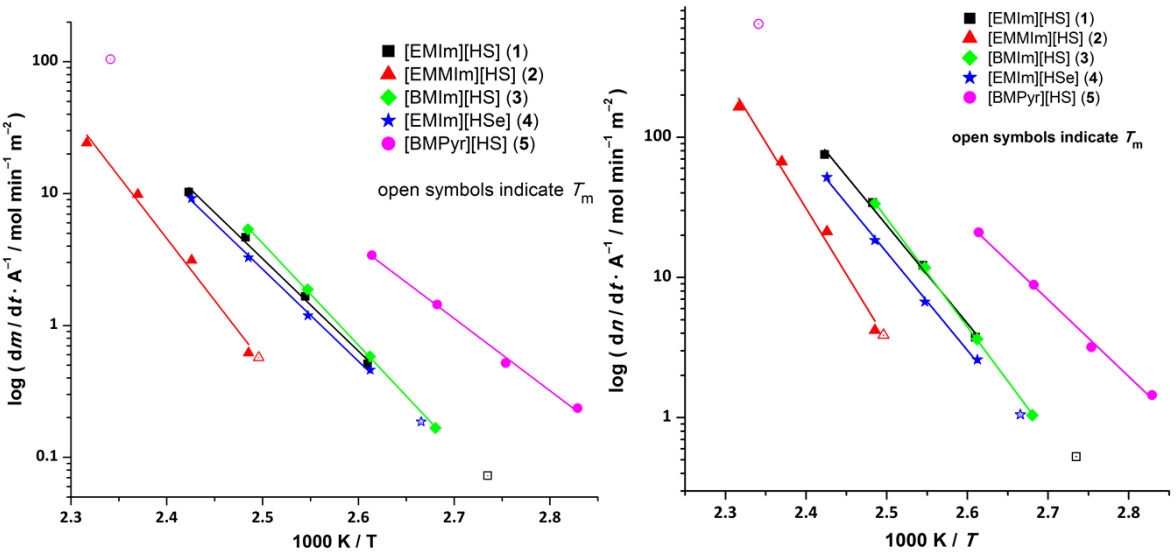

Figure S11. Arrhenius plots of the mass loss rate (left) and the molar loss rates (right) per unit area of compounds 1 to 5, the melting temperature of [BMIm][HS] lies outside of the current graph borders at 3.05.

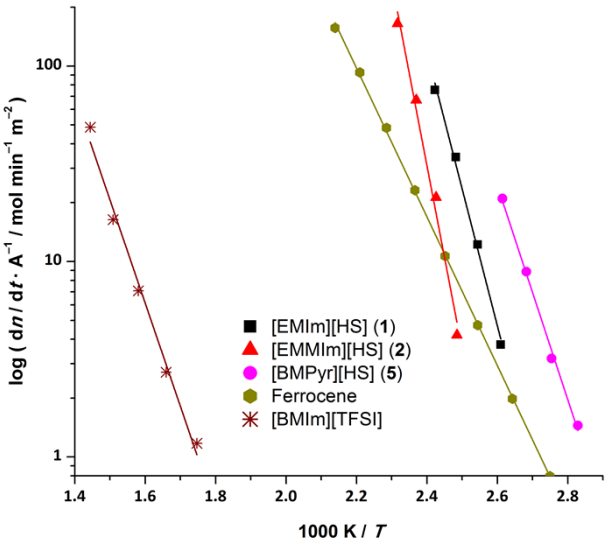

Figure S12. Arrhenius plots of the molar loss rates per unit area, comparing the hydrosulphides 1, 2, 5, ferrocene and [BMIm][TFSI].

7. Computational methods

Structure optimisation for the most stable conformations of [EMIm][HS] single ion pairs (SIPs) in the gas phase (figure S13) as well as reaction path search for the decomposition processes occurring during the vaporisation were studied with the quantum chemistry programme Gaussian 09.[18] These calculations for gas phase structures were performed within density functional theory on a BP86/def2-TZVP level.[19] Molecular structures for stationary points on the Born-Oppenheimer hypersurface were obtained such that the root mean square (RMS) of all force components with respect to internal coordinates dropped below $10^{-5}\,E_h \cdot a_0^{-1}$ and $10^{-5}\,E_h \cdot rad^{-1}$. Convergence criteria in the self-consistent field (SCF) procedure were that RMS changes in the density matrix between two successive SCF cycles remained below 10^{-8}. The integration scheme is "UltraFine", i.e. a pruned (99, 590) grid for the numerical integration step involved in the construction of the exchange correlation potential. All stationary points were characterised by harmonic vibrational frequency calculations and minimum energy reaction paths were obtained *via* the steepest gradient descent approach. To identify the type of bonding interaction present in the SIP b) (figure S13), the program AIMALL[20] was employed to perform the QTAIM (Quantum Theory of Atoms in Molecules) analysis according to R. F. W. Bader.[21] Additionally to that, a natural bond orbital analysis[22] in NBO 3.1[23] and an energy decomposition analysis (EDA)[24] in ADF[25] were performed.

Calculations concerning cohesive energies were performed with the Vienna Ab initio Simulation Package (VASP). The experimental crystal structures of compounds **1** and **3,** which were determined in the course of this work, were used as input. The structure of **1** is submitted with this publication (*vide supra*). The CIF files of all structures have been deposited with the CCDC and can be obtained under CCDC 1414150 to 1414153. Structure optimisations were performed for monoclinic [EMIm][HS] (**1**) and [EMIm][[HSe] (**4**) and orthorhombic [EMMIm][HS] (**2**) and [BMIm][HS] (**3**) crystal structures, as well as for single ion pairs in the gas phase. These calculations were performed within the non-spin polarised density functional theory and the Generalised Gradient Approximation PBE (GGA-PBE)[26] together with the projector-augmented-wave (PAW) method[27] as implemented in the Vienna Ab initio Simulation Package (VASP.5.3.5).[28] A kinetic energy cut-off of 480 eV is used for convergence of the total energy within 1 meV. Gamma k-point meshes of 4 x 4 x 6 for [EMMIm][HS], 4 x 6 x 4 for [EMIm][HSe] and 4 × 4 × 4 for the two other crystal unit cells are used for Brillouin zone integration to calculate the electronic ground states. Long-range

van-der-Waals interactions were accounted for by employing the zero damping DFT-D3 scheme of Grimme.[29]

Cohesive energies (E_{coh}) are assumed to be approximately equal to the sublimation enthalpies (ΔH_{sub}) and were calculated using the relation

$$\Delta H_{sub} \approx E_{coh} = E_{unit} - E_{bulk}/N_{unit},$$

where E_{unit} is the energy of a single ion pair in the most stable conformation in vacuum and E_{bulk} is the energy per unit cell of the respective salt. N_{unit} is the number of formula units in the simulation cell of the given crystalline structure ($N_{Unit} = 8$ for [EMMIm][HS], and $N_{Unit} = 4$ for the others). E_{unit} was calculated in a simulation cell, which is sufficiently large to avoid artificial interactions between a SIP and its periodic images. For the same purpose, the cut-off radius of the force field within the context of the PBE-D3 scheme was reduced. Equilibrium structures were obtained using the conjugate gradient optimisation. All atoms were fully relaxed until the change in forces on the ionic displacements was below 0.01 eV/Å. No other constraints were imposed for structure optimisation calculations in the bulk systems. The optimized lattice parameters (a, b, c, β) for the crystal structures (table S3) show a slight deviation from the experimental values.

Table S3. Strucutral parameters of the unit cells of compounds 1 to 4 after structure optimisation (exprimental values in parenthesis).

Compound	a/ Å	b/ Å	c/ Å	β/°
[EMIm][HS] (**1**)	8.58 (8.60)	7.54 (7.67)	12.67 (12.76)	107.7 (107.9)
[EMMIm][HS] (**2**)	7.84 (8.02)	13.32 (13.43)	16.46 (16.64)	- -
[BMIm][HS] (**3**)	9.84 (9.91)	12.04 (12.14)	8.16 (8.23)	- -
[EMIm][HSe] (**4**)	8.57 (8.60)	7.60 (7.78)	13.20 (13.30)	108.4 (108.2)

7.1 Gas phase structure optimisation of [EMIm][HS] single ion pairs

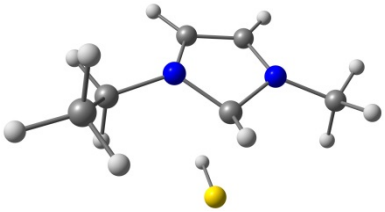

a) E_{rel} = 0.0 kJ·mol^{-1}

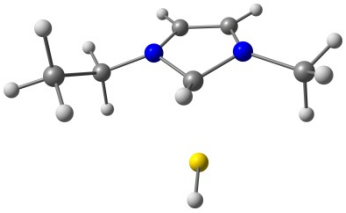

b) E_{rel} = 1.9 kJ·mol^{-1}

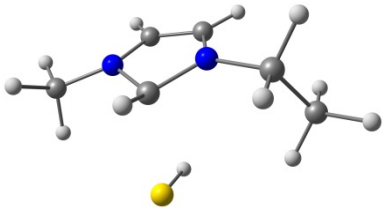

c) E_{rel} = 4.0 kJ·mol^{-1}

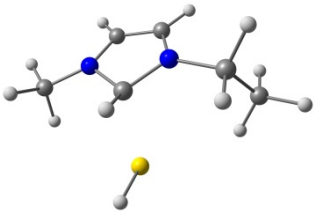

d) E_{rel} = 5.7 kJ·mol^{-1}

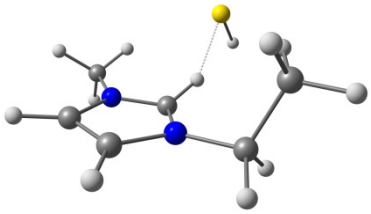

e) E_{rel} = 16.9 kJ·mol^{-1}
D(C−H···S): 3.07 Å
<(C−H···S): 149.9°

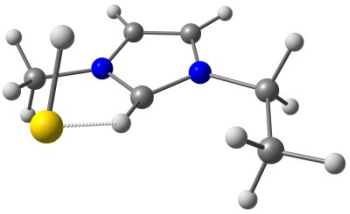

f) E_{rel} = 18.3 kJ·mol^{-1}
D(C−H···S): 3.08 Å
<(C−H···S): 152.7°

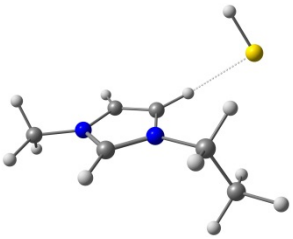

g) E_{rel} = 53.5 kJ·mol^{-1}
D(C−H···S): 3.21 Å
<(C−H···S): 146.8°

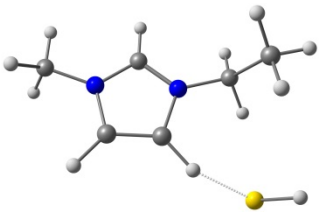

h) E_{rel} = 54.6 kJ·mol^{-1}
D(C−H···S): 3.21 Å
<(C−H···S): 144.8°

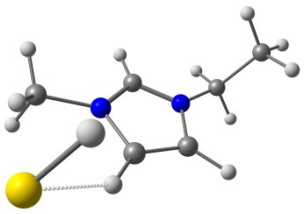

i) E_{rel} = 54.6 kJ·mol^{-1}
D(C−H···S): 3.19 Å
<(C−H···S): 145.8°

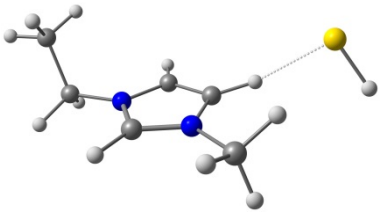

j) E_{rel} = 55.4 kJ·mol^{-1}
D(C−H···S): 3.20 Å
<(C−H···S): 143.9°

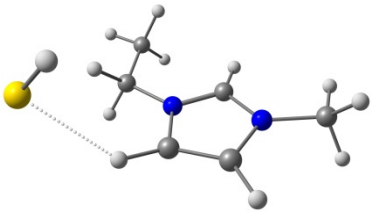

k) E_{rel} = 58.5 kJ·mol^{-1}
D(C−H···S): 3.19 Å
<(C−H···S): 136.2°

Figure S13. Most stable ion pairs of [EMIm][HS] (without ZPE correction).

Table S4. Total electronic energies of the [EMIm][HS] SIPs (without ZPE correction).

	E/ E_h	E_{rel}/ kJ·mol^{-1}
(a)	−743.703593	0.0
(b)	−743.702876	1.9
(c)	−743.702057	4.0
(d)	−743.701422	5.7
(e)	−743.697161	16.9
(f)	−743.696625	18.3
(g)	−743.683208	53.5
(h)	−743.682816	54.6
(i)	−743.682783	54.6
(j)	−743.682511	55.4
(k)	−743.681308	58.5

7.2 S_N2 reactions and carbene formation as decomposition pathways

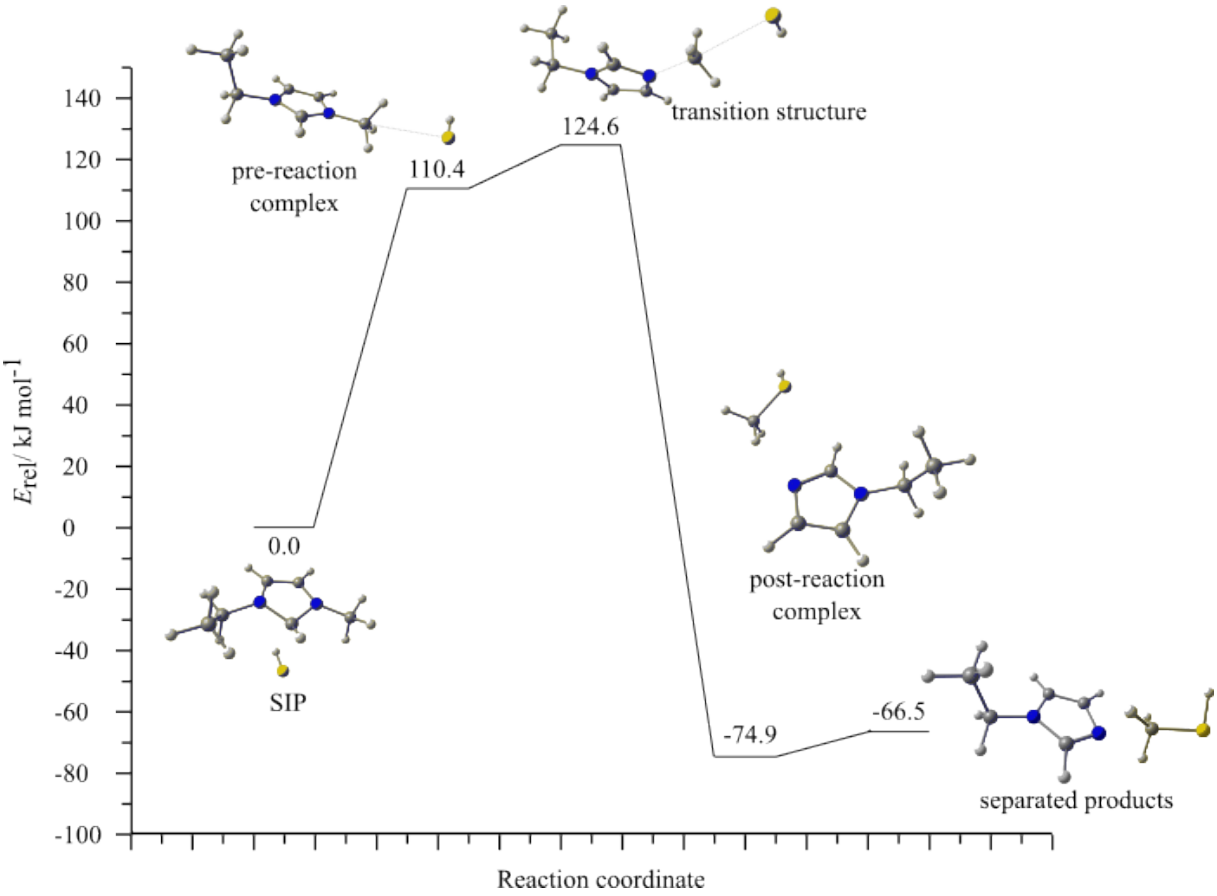

Figure S14. Decomposition of [EMIm][HS] by nucleophilic attack at the methyl group.

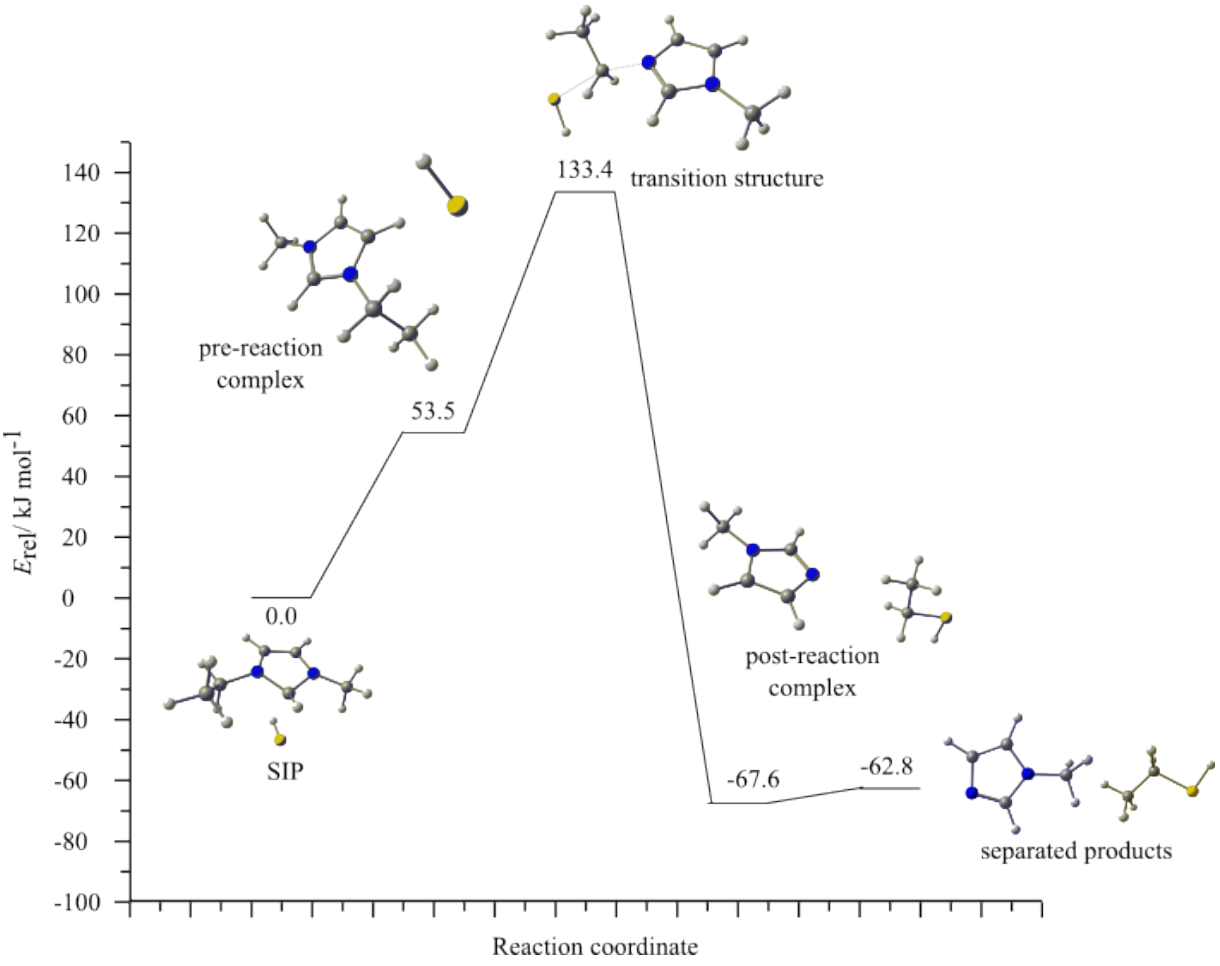

Figure S15. Decomposition of [EMIm][HS] by nucleophilic attack at the ethyl group.

Table S5. Total electronic energies of the S_N2-type reactions (without ZPE correction).

Attack at the methyl group	E/ E_h	E_{rel}/ kJ·mol^{-1}
Ion pair (most stable one)	−743.703593	0.0
Pre-reaction complex	−743.661534	110.4
Transition structure	−743.656123	124.6
Post-reaction complex	−743.732113	−74.9
Products (separated)	−743.728935	−66.5
Attack at the ethyl group		
Ion pair (most stable one)	−743.703593	0.0
Pre-reaction complex	−743.683208	53.5
Transition structure	−743.652775	133.4
Post-reaction complex	−743.729330	−67.6
Products (separated)	−743.727514	−62.8

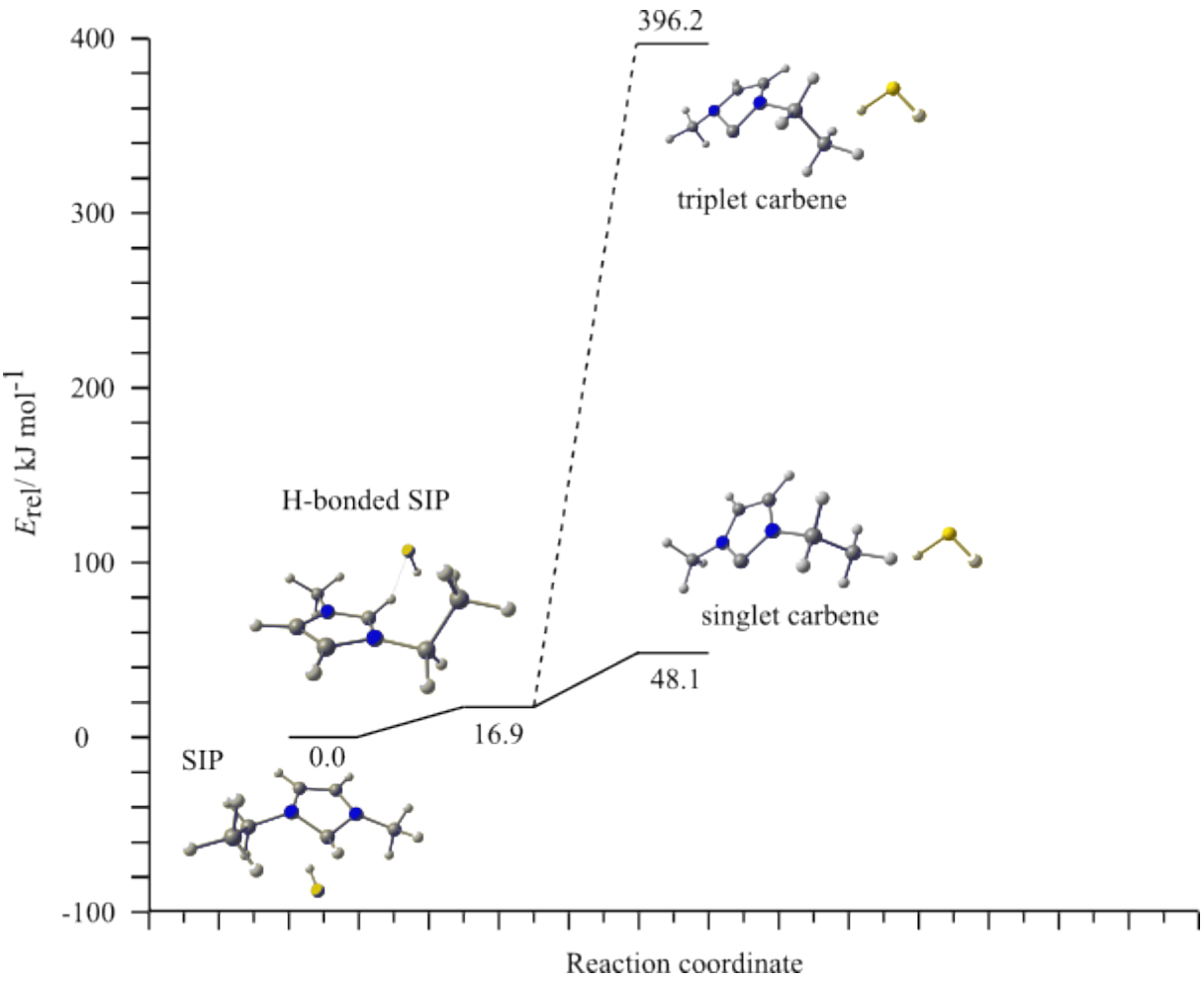

Figure S16. Energy profile of the carbene formation.

Table S6. Total electronic energies of the carbene formation (without ZPE correction).

Attack at the methyl group	E/ E_h	E_{rel}/ kJ·mol^{-1}
Ion pair (most stable one)	−743.703593	0.0
H−bonded SIP	−743.697161	16.9
Singlet carbene	−743.685269	48.1
Triplet carbene	−743.552676	396.2

7.3 Formation of 1-ethyl-3-methylimidazole-2-thione

As already noted by Hollóczki *et al.* a neutral thiol species **A**, resulting from nucleophilic attack of the hydrosulphide at the C2 position (scheme S2) cannot be stabilised.[30] This forced reaction is accompanied by slight increase in energy by about 28.2 kJ·mol^{-1}, with the corresponding structure not being a stationary point on the potential energy hypersurface.

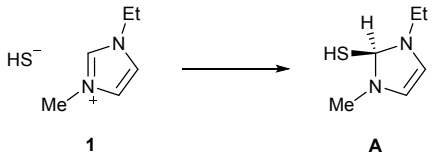

Scheme S2. Formation of an imidazole-2-thiole by nucleophilic attack of HS^- at the C2-carbon.

The reaction becomes thinkable if another hydrosulphide anion is included, which will act as Brønstedt base and concertedly deprotonates the thiole to anion **B** (scheme S3). According to DFT calculations, in the gas phase this reaction would be accompanied by an overall energy loss of −6.3 kJ·mol^{-1}.

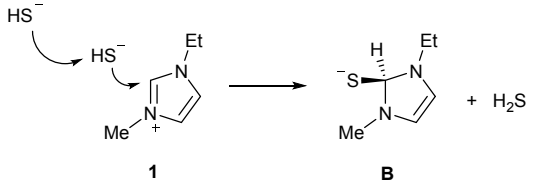

Scheme S3. Formation of an imidazole-2-thiolate by nucleophilic attack of HS^- at the C2-carbon and concerted deprotonation by anonther hydrosulphide anion.

Thiolate **B** will act as a strong hydride donor and reacts with the strongest acid present in the system, which is again the hydrosulphide anion (pK_a (HS^-) ≈ 14, pKa ($[EMIm]^+$) = 23).[31] Thiole **A** will certainly show a lower pK_a value, but its questionable existence and, if at all, very low abundance renders it an improbable reaction partner. The forming sulphide dianion will immediately attack the next [EMIm] cation initiating an autocatalytic cycle (scheme S4). The overall energy balance of the reaction is computed to be exothermic by −51.01 kJ/mol.

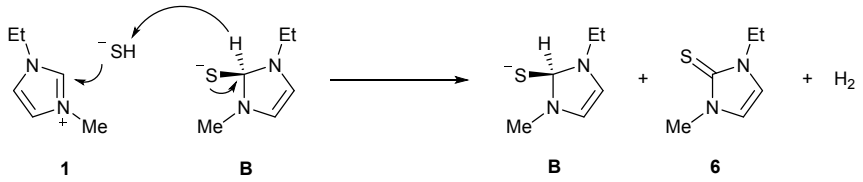

Scheme S4. Generation of the thione 6 and initiation of an autocatalytic decomposition cycle.

Table S7 summarises the computed energies of the single components and table S8 reports the total energies of the reactions depicted in schemes S2 to S4.

Table S7. Total electronic energies of the single components (without ZPE correction).

	E/ E_h
Most stable SIP [EMIm][HS]	−743.703593
Thiole **A**	−743.692868
Hydrosulphide anion (HS^-)	−398.871600
Thiolate **B**	−743.128954
Hydrogen sulphide (H_2S)	−399.448640
Thione **6**	−742.545439
Hydrogen (H_2)	−1.177586

Table S8. Total energies of the reactions depicted in schemes S2 to S4.

Reaction of scheme S2	E/ E_h	ΔE_{rel}/ kJ·mol^{-1}
[EMIm][HS] SIP	−743.703593	0.0
Thiole **A**	−743.692868	28.2
Reaaction of scheme S3		
Separated reactants	−1142.575196	0.0
Separated products	−1142.577594	−6.3
Reaction of scheme S4		
Separated reactants	−1486.832550	0.0
Separated products	−1486.851979	−51.0

7.4 Analysis of the bonding interaction in the single ion pair b) and thiol A

The formation of a 1-ethyl-3-methylimidazol-2-thiole was anticipated as a possible intermediate during the generation of the respective thione. However, the structure with separated ion and a C−S distance of 2.26 Å (equivalent to ion pair b) of figure S13) is more stable than the covalently bound molecule, where the bond length was fixed to 1.82 Å, which was assumed a typical C−S single bond length. Figure S17 visualises the relative energy change with varying C−S distance.

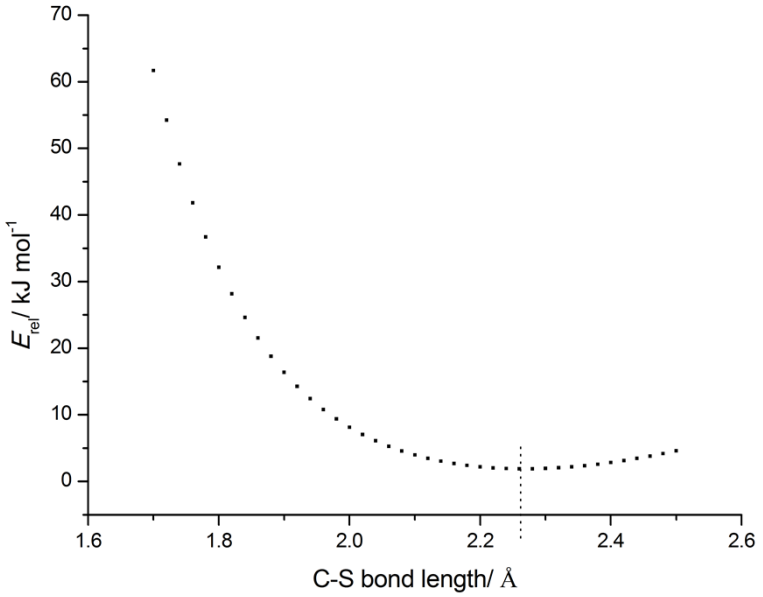

Figure S17. Relative energy of the [EMIm][HS] SIP b) in dependency of the C−S distance (E_{rel} = 0 corresponds to the most stable SIP a) of figure S13).

Comparing the bond length with other ionic pairs, where the anion is not located above the ring-system of the imidazolium, the abnormality gets fortified. There, the C−S bond length is always larger than 3 Å, which indicates that ion pair b) has a more covalent character than other ionic pairs like the H-bonded ion pair e). To identify the type of bonding interaction present in the structure b) a Bader analysis,[21] a natural bond orbital analysis[22] and an energy

decomposition analysis[24] were performed, comparing structure b), methanethiol and sodium hydrosulphide. A bond critical point was found between sulphur and the carbon of interest, with an electron (charge) density $\rho = 7.64 \cdot 10^{-2}\ (-e) \cdot a_0^{-3}$ and a Laplacian of the electron density of $\nabla^2\rho = 3.63 \cdot 10^{-2}\ (-e) \cdot a_0^{-5}$. The criterion for a covalent bonding interaction is that $\rho/(-e) \cdot a_0^{-3}$ should be higher than 0.2 and $\nabla^2\rho/(-e) \cdot a_0^{-5}$ should be negative.[32] This indicates the carbon-sulphur interaction to be mostly of ionic character (figure S18). For methanethiol the values $\rho = 1.73 \cdot 10^{-1}\ (-e) \cdot a_0^{-3}$ and $\nabla^2\rho = -2.57 \cdot 10^{-1}\ (-e) \cdot a_0^{-5}$ and for sodium hydrosulphide the values $\rho = 3.07 \cdot 10^{-2}\ (-e) \cdot a_0^{-3}$ and $\nabla^2\rho = 1.38 \cdot 10^{-1}\ (-e) \cdot a_0^{-5}$ were calculated. These fit to the expectations of mainly covalent and ionic interactions, respectively.

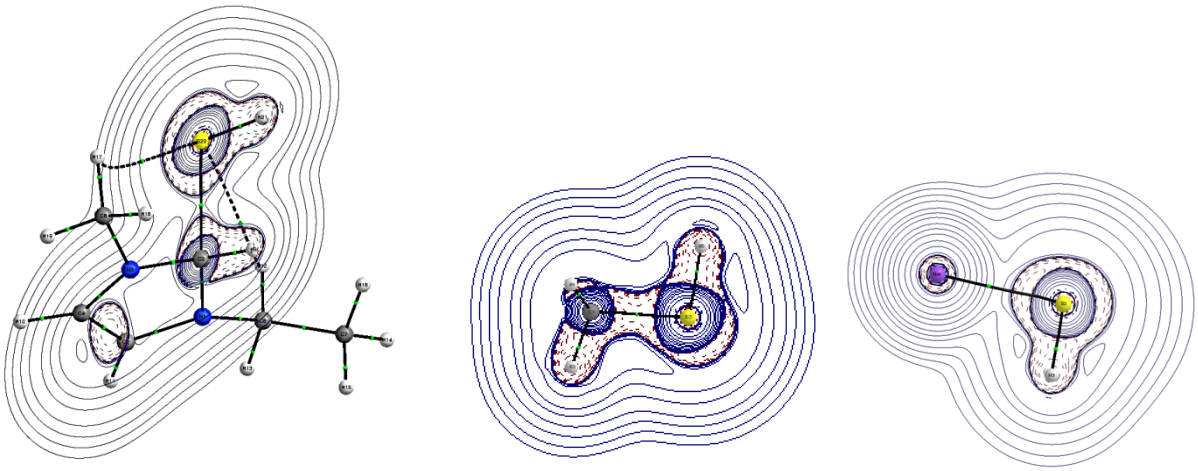

Figure S18. Bader analysis of the ion pair b), methanethiol and sodium hydrosulphide (from left to right).

The NBO analysis (figure S19), in contrast reveals a σ-like bond orbital, indicating a covalent bond. It is overt, that the orbital is highly deformed; the electron density is located more on the sulphur atom due to its higher electronegativity.

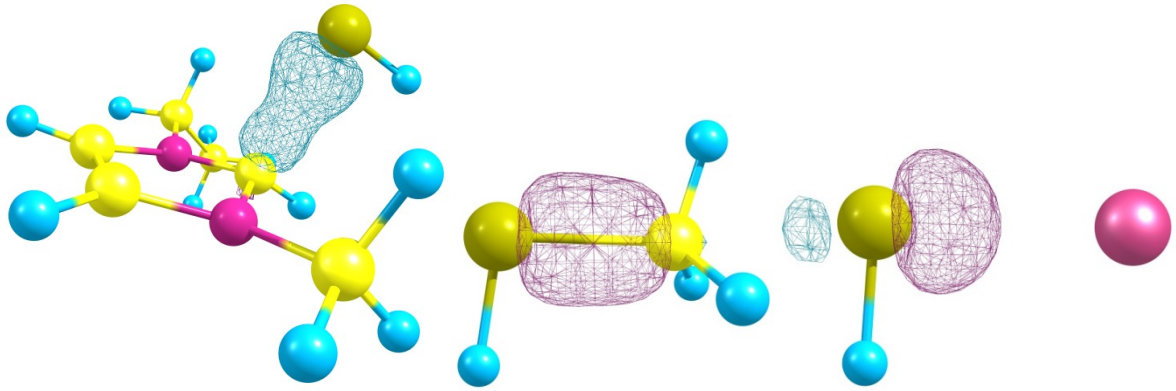

Figure S19. Natural bonding orbitals of the ion pair b), methanethiol and sodium hydrosulphide (from left to right) .

The energy decomposition analysis (EDA) of the three compounds finally confirms an intermediate state between a covalent bond and an ionic character of the interaction. The H−bonded ion pair e) in comparison shows a significantly higher electrostatic contribution (Tabel S9).

Table S9. Energy decomposition analysis of Ion pairs b), e), methanethiol and sodium hydrosulphide.

	Ion pair b)	Ion pair e)	Methanethiol	Sodium hydrosulphide
E_{total}/ kJ•mol^{-1}	−116.0	−102.8	−285.1	−133.7
E_{pauli}/ kJ•mol^{-1}	127.2	48.9	187.9	30.4
$E_{el.static}$/ kJ•mol^{-1}	−160.5	−110.3	−223.8	−146.5
	(66.0%)	(72.7%)	(47.3%)	(89.3%)
$E_{orbital}$/ kJ•mol^{-1}	−82.8	−41.4	−249.2	−17.6
	(34.0%)	(27.3%)	(52.7%)	(10.7%)
E_{diss}/ kJ•mol^{-1}	99.2	95.8		

Also the bond indices of the carbon-sulphur bond according to Wiberg[22a] produce an intermediate value for the ion pair b) (BI = 0.5681). The values for methyl-thiol (BI = 1.0486) and sodium hydrosulphide (BI = 0.3576) clearly indicate covalent and ionic interactions, respectively.

8. EI-MS-Spectra

[EMIm][HS], 1

Data:150422_EI_649_Su
Comment:
Description:
Ionization Mode:EI+
History:Centroid[Peak Detect[Centroid,90,Area];Smooth[5]];Average(MS[1] 3.44..3.50)

Acquired:2015-04-23 1:09:39 PM
Operator:AccuTOF
m/z Calibration File:Pos_800-20150310
Created:12:00:00 AM
Created by:

Charge number:1 Tolerance:5.00[mDa]
Element:^{12}C:2 .. 2, ^{1}H:4 .. 4, ^{11}B:0 .. 0, ^{79}Br:0 .. 0, ^{14}N:0 .. 0, ^{16}O:2 .. 2

Unsaturation Number:-1.5 .. 20.0 (Fraction:Both)

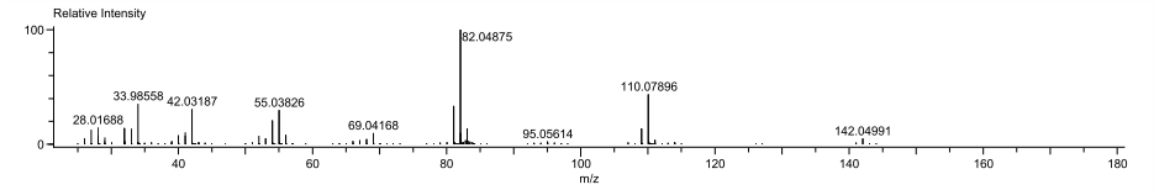

H_2S

Chemical Formula: H_2S
Exact Mass: 33,9877

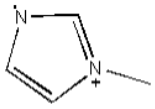

Chemical Formula: $C_4H_6N_2^+$
Exact Mass: 82,0525

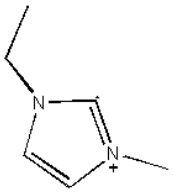

Chemical Formula: $C_6H_{10}N_2^{\bullet+}$
Exact Mass: 110,0838

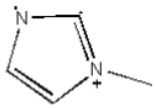

Chemical Formula: $C_4H_5N_2^{\bullet+}$
Exact Mass: 81,0447

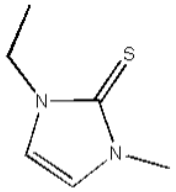

Chemical Formula: $C_6H_{10}N_2S$
Exact Mass: 142,0565

Data:150422_EI_649_Su
Comment:
Description:
Ionization Mode:EI+
History:Centroid[Peak Detect[Centroid,90,Area];Smooth[5]];Average(MS[1] 2.64..2.70)

Acquired:2015-04-23 1:09:39 PM
Operator:AccuTOF
m/z Calibration File:Pos_800-20150310
Created:2015-04-27 11:32:44 AM
Created by:Administrator

Charge number:1 Tolerance:5.00[mDa]
Element:^{12}C:0 .. 0, ^{1}H:2 .. 2, ^{11}B:0 .. 0, ^{79}Br:0 .. 0, ^{14}N:0 .. 0, ^{16}O:0 .. 0, ^{32}S:1 .. 1

Unsaturation Number:-1.5 .. 20.0 (Fracti...

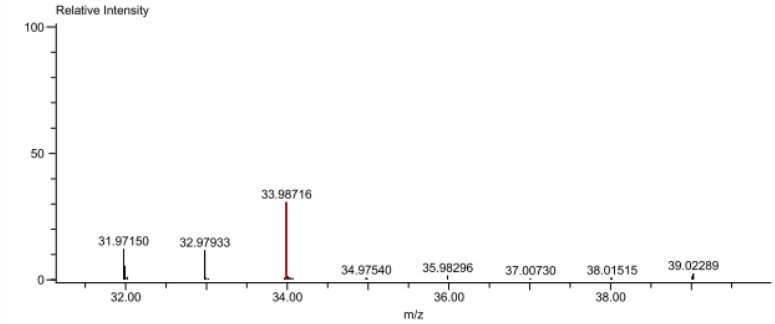

Composition:H_2S
Mono Isotopic Mass:33.98772
Average Mass:34.08188
Description:

Created:2015-04-27 11:32:45 AM
Nominal Mass:34
Created by:Administrator

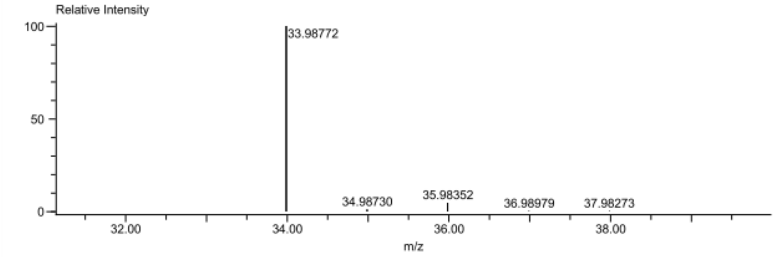

Mass	Intensity	Relative Intensity	Calc. Mass	Mass Difference [mDa]	Mass Difference [ppm]	Possible Formula
33.98716	311223.49	30.54	33.98772	-0.56	-16.53	$^{1}H_2{}^{32}S_1$

Data:150422_EI_649_Su
Comment:
Description:
Ionization Mode:EI+
History:Centroid[Peak Detect[Centroid,30,Area]];Average(MS[1] 3.41..3.48)

Acquired:4/23/2015 1:09:39 PM
Operator:AccuTOF
m/z Calibration File:Pos_800-20150310
Created:6/25/2015 9:48:09 AM
Created by:AccuTOF

Charge number:1 Tolerance:2.00[mDa]
Element:^{12}C:0 .. 6, ^{1}H:0 .. 10, ^{11}B:0 .. 0, ^{79}Br:0 .. 0, ^{14}N:0 .. 2, ^{16}O:0 .. 0, ^{32}S:0 .. 1

Unsaturation Number:-1.5 .. 20.0 (Fraction:Both)

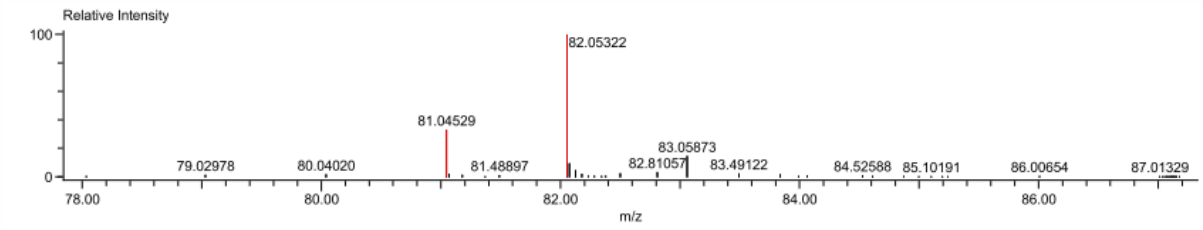

Composition:$C_4H_6N_2$
Mono Isotopic Mass:82.05310 Average Mass:82.10392
Description:

Created:6/25/2015 9:50:05 AM
Nominal Mass:82
Created by:AccuTOF

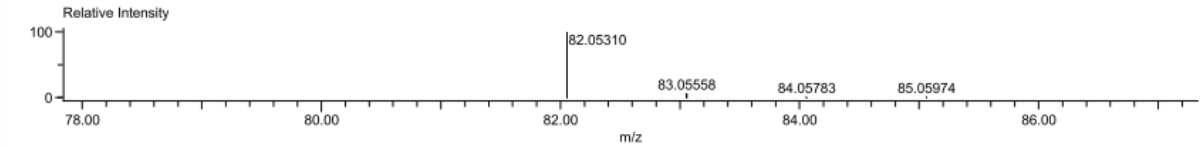

Mass	Intensity	Relative Intensity	Calc. Mass	Mass Difference [mDa]	Mass Difference [ppm]	Possible Formula
81.04529	719664.84	32.60	81.04527	0.01	0.15	$^{12}C_4{}^{1}H_5{}^{14}N_2$
82.05322	2207417.04	100.00	82.05310	0.12	1.51	$^{12}C_4{}^{1}H_6{}^{14}N_2$
142.05705	103838.01	4.70	142.05647	0.58	4.07	$^{12}C_8{}^{1}H_{10}{}^{14}N_2{}^{32}S_1$

Data:150422_EI_649_Su
Comment:
Description:
Ionization Mode:EI+
History:Centroid[Peak Detect[Centroid,90,Area];Smooth[5]];Average(MS[1] 2.64..2.70)

Acquired:2015-04-23 1:09:39 PM
Operator:AccuTOF
m/z Calibration File:Pos_800-20150310
Created:2015-04-27 11:14:58 AM
Created by:Administrator

Charge number:1 Tolerance:5.00[mDa]
Element:^{12}C:6 .. 6, ^{1}H:10 .. 10, ^{11}B:0 .. 0, ^{79}Br:0 .. 0, ^{14}N:2 .. 2, ^{16}O:0 .. 0

Unsaturation Number:-1.5 .. 20.0 (Fracti.

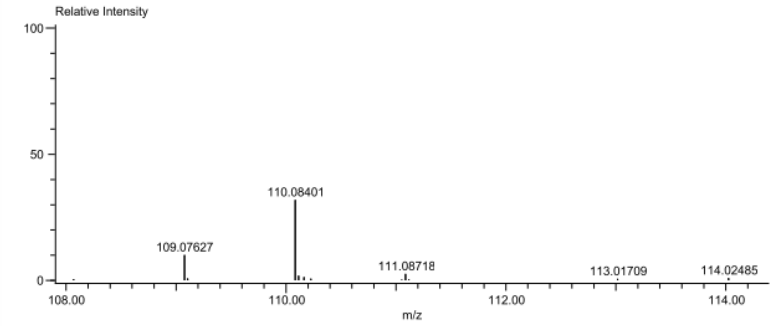

Composition:$C_6H_{10}N_2$
Mono Isotopic Mass:110.08440 Average Mass:110.15708
Description:

Created:2015-04-27 11:28:48 AM
Nominal Mass:110
Created by:Administrator

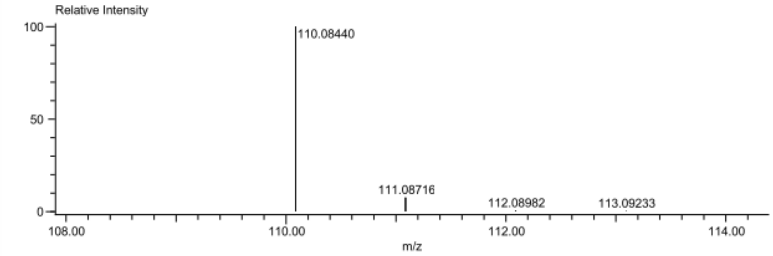

Mass	Intensity	Relative Intensity	Calc. Mass	Mass Difference [mDa]	Mass Difference [ppm]	Possible Formula
110.08401	323000.26	31.70	110.08440	-0.38	-3.49	$^{12}C_6{}^{1}H_{10}{}^{14}N_2$

Data:150422_EI_649_Su
Comment:
Description:
Ionization Mode:EI+
History:Centroid[Peak Detect[Centroid,30,Area]];Average(MS[1] 3.41..3.48)

Acquired:4/23/2015 1:09:39 PM
Operator:AccuTOF
m/z Calibration File:Pos_800-20150310
Created:6/25/2015 9:48:09 AM
Created by:AccuTOF

Charge number:1 Tolerance:2.00[mDa]
Element:^{12}C:0 .. 6, ^{1}H:0 .. 10, ^{11}B:0 .. 0, ^{79}Br:0 .. 0, ^{14}N:0 .. 2, ^{16}O:0 .. 0, ^{32}S:0 .. 1

Unsaturation Number:-1.5 .. 20.0 (Fraction:Both)

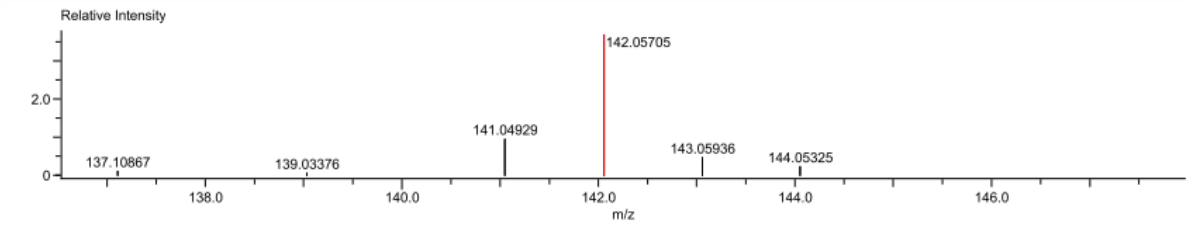

Composition:$C_6H_{10}N_2S$
Mono Isotopic Mass:142.05647 Average Mass:142.22308
Description:

Created:6/25/2015 9:50:11 AM
Nominal Mass:142
Created by:AccuTOF

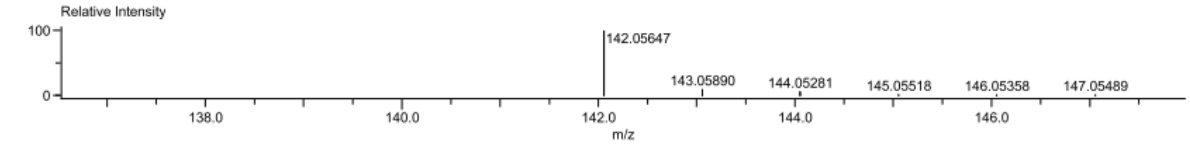

Mass	Intensity	Relative Intensity	Calc. Mass	Mass Difference [mDa]	Mass Difference [ppm]	Possible Formula
81.04529	719664.84	32.60	81.04527	0.01	0.15	$^{12}C_4{}^{1}H_5{}^{14}N_2$
82.05322	2207417.04	100.00	82.05310	0.12	1.51	$^{12}C_4{}^{1}H_6{}^{14}N_2$
142.05705	103838.01	4.70	142.05647	0.58	4.07	$^{12}C_8{}^{1}H_{10}{}^{14}N_2{}^{32}S_1$

[EMMIm][HS], 2

Data:150422_EI_650_Su
Comment:
Description:
Ionization Mode:EI+
History:Centroid[Peak Detect[Centroid,30,Area]];Average(MS[1] 0.69..0.86)

Acquired:4/23/2015 2:25:10 PM
Operator:AccuTOF
m/z Calibration File:Pos_800-20150310
Created:6/25/2015 10:06:22 AM
Created by:AccuTOF

Charge number:1 Tolerance:2.00[mDa]
Element:^{12}C:0 .. 7, ^{1}H:0 .. 12, ^{11}B:0 .. 0, ^{79}Br:0 .. 0, ^{14}N:0 .. 2, ^{16}O:0 .. 0, ^{32}S:0 .. 1

Unsaturation Number:-1.5 .. 20.0 (Fraction:Both)

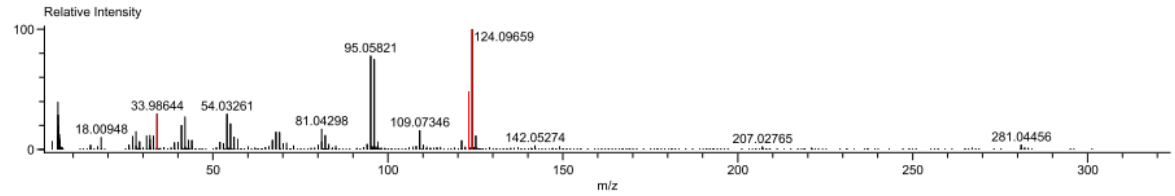

Mass	Intensity	Relative Intensity	Calc. Mass	Mass Difference [mDa]	Mass Difference [ppm]	Possible Formula
33.98644	472162.24	29.20	33.98772	-1.28	-37.54	$^{1}H_2{}^{32}S_1$
123.08888	769036.08	47.56				
124.09659	1616992.66	100.00				

H_2S

Chemical Formula: H_2S
Exact Mass: 33,9877

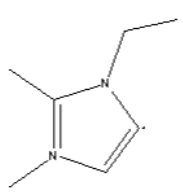

Chemical Formula: $C_7H_{12}N_2^{\bullet}$
Exact Mass: 124,1000

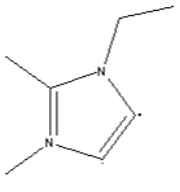

Chemical Formula: $C_7H_{11}N_2^{2\bullet}$
Exact Mass: 123,0922

Data:150422_EI_650_Su
Comment:
Description:
Ionization Mode:EI+
History:Centroid[Peak Detect[Centroid,30,Area]];Average(MS[1] 0.69..0.86)

Acquired:4/23/2015 2:25:10 PM
Operator:AccuTOF
m/z Calibration File:Pos_800-20150310
Created:6/25/2015 10:06:22 AM
Created by:AccuTOF

Charge number:1 Tolerance:2.00[mDa]
Element:^{12}C:0 .. 7, ^{1}H:0 .. 12, ^{11}B:0 .. 0, ^{79}Br:0 .. 0, ^{14}N:0 .. 2, ^{16}O:0 .. 0, ^{32}S:0 .. 1

Unsaturation Number:-1.5 .. 20.0 (Fraction:Both)

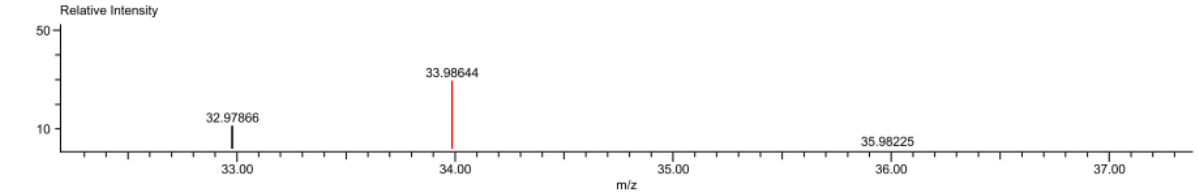

Composition:H_2S
Mono Isotopic Mass:33.98772 Average Mass:34.08188
Description:

Created:6/25/2015 10:08:56 AM
Nominal Mass:34
Created by:AccuTOF

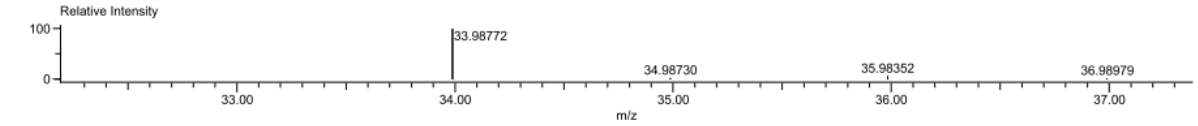

Mass	Intensity	Relative Intensity	Calc. Mass	Mass Difference [mDa]	Mass Difference [ppm]	Possible Formula
33.98644	472162.24	29.20	33.98772	-1.28	-37.54	$^{1}H_2{}^{32}S_1$
123.08888	769036.08	47.56				
124.09659	1616992.66	100.00				

Data:150422_EI_650_Su
Comment:
Description:
Ionization Mode:EI+
History:Centroid[Peak Detect[Centroid,30,Area]];Average(MS[1] 1.10..1.44)

Acquired:23.04.2015 14:25:10
Operator:AccuTOF
m/z Calibration File:Pos_800-20150310
Created:27.05.2015 12:21:50
Created by:

Charge number:1 Tolerance:100.00[ppm], 5.00 .. 15.00[mDa]
Element:^{12}C:7 .. 7, ^{1}H:12 .. 12, ^{11}B:0 .. 0, ^{79}Br:0 .. 0, ^{14}N:2 .. 2, ^{16}O:0 .. 0, ^{28}Si:0 .. 0, ^{29}Si:0 .. 0

Unsaturation Number:-1.5 .. 20.0 (Fraction:Both)

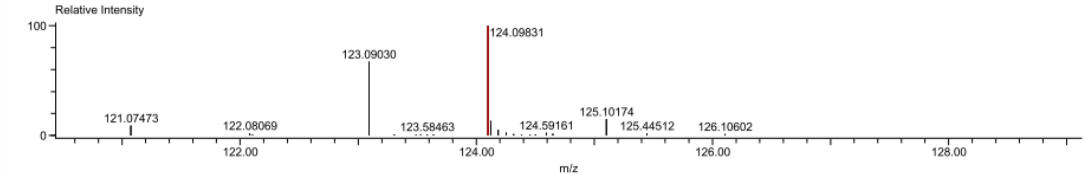

Composition:$C_7H_{12}N_2$
Mono Isotopic Mass:124.10005 Average Mass:124.18366
Description:

Created:27.05.2015 12:21:51
Nominal Mass:124
Created by:

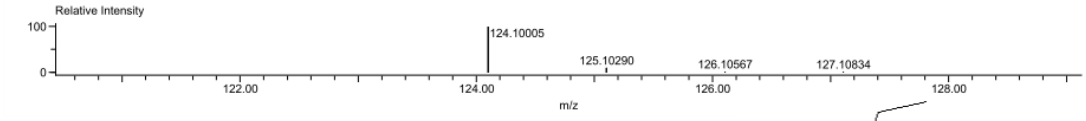

Mass	Intensity	Relative Intensity	Calc. Mass	Mass Difference [mDa]	Mass Difference [ppm]	Possible Formula
124.09831	2455519.43	100.00	124.10005	-1.74	-14.01	$^{12}C_7{}^{1}H_{12}{}^{14}N_2$

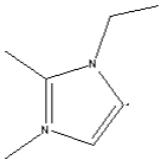

Chemical Formula: $C_7H_{12}N_2^{\bullet}$
Exact Mass: 124,1000

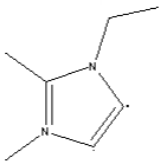

Chemical Formula: $C_7H_{11}N_2^{2\bullet}$
Exact Mass: 123,0922

[BMIm][HS], 3

Data:150511_EI_701_Su
Comment:
Description:
Ionization Mode:EI+
History:Average(MS[1] 0.36..0.39)-1*Average(MS[1] 0.02..0.24),#0-

Acquired:2015-06-12 10:04:40 AM
Operator:AccuTOF
m/z Calibration File:Pos_800-20150601
Created:2015-06-15 1:30:44 PM
Created by:Administrator

Charge number:1 Tolerance:5.00[ppm], 5.00 .. 15.00[mDa]
Element:^{12}C:0 .. 8, ^{1}H:0 .. 14, ^{11}B:0 .. 0, ^{14}N:0 .. 2, ^{16}O:0 .. 2, ^{32}S:0 .. 1

Unsaturation Number:-1.5 .. 20.0 (Fraction:Both)

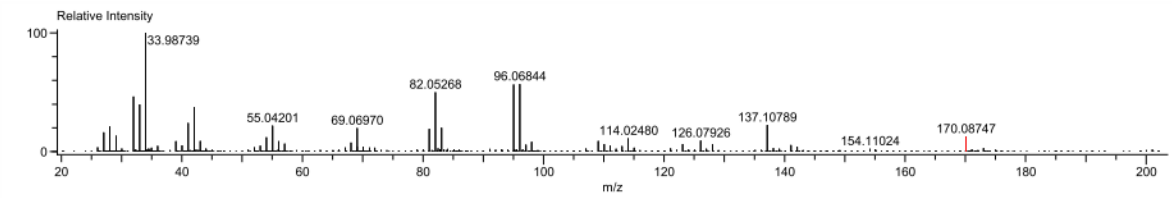

Mass	Intensity	Calc. Mass	Mass Difference [mDa]	Possible Formula
170.08747	111288.84	170.08777	-0.30	$^{12}C_8{}^{1}H_{14}{}^{14}N_2{}^{32}S_1$

Data:150511_EI_701_Su
Comment:
Description:
Ionization Mode:EI+
History:Average(MS[1] 1.41..1.49)

Acquired:6/12/2015 10:04:40 AM
Operator:AccuTOF
m/z Calibration File:Pos_800-20150601
Created:6/25/2015 10:25:59 AM
Created by:AccuTOF

Charge number:1 Tolerance:2.00[mDa]
Element:^{12}C:0 .. 8, ^{1}H:0 .. 13, ^{11}B:0 .. 0, ^{79}Br:0 .. 0, ^{14}N:0 .. 2, ^{16}O:0 .. 0, ^{32}S:0 .. 1

Unsaturation Number:-1.5 .. 20.0 (Fraction:Both)

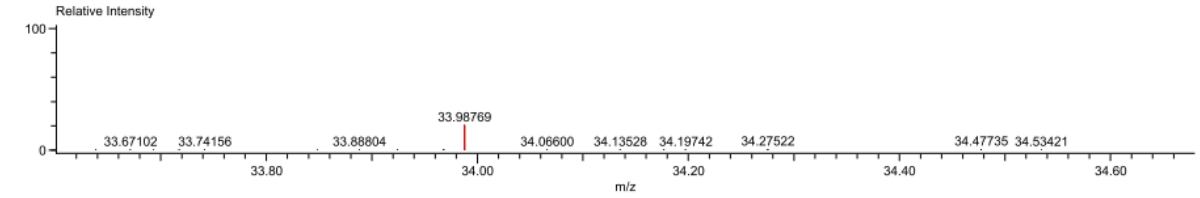

Composition:H_2S
Mono Isotopic Mass:33.98772
Description:

Average Mass:34.08188

Created:6/25/2015 10:27:13 AM
Nominal Mass:34
Created by:AccuTOF

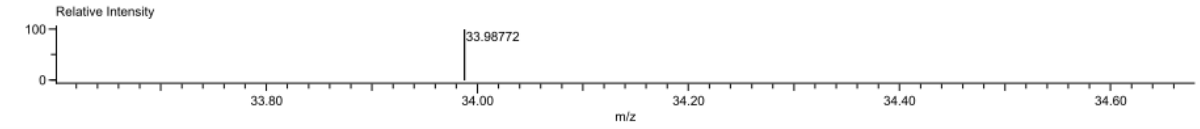

Mass	Intensity	Relative Intensity	Calc. Mass	Mass Difference [mDa]	Mass Difference [ppm]	Possible Formula
33.98769	513486.09	20.14	33.98772	-0.03	-1.00	$^{1}H_2{}^{32}S_1$
95.06139	2017161.45	79.12	95.06092	0.46	4.88	$^{12}C_5{}^{1}H_7{}^{14}N_2$
96.06915	2549640.44	100.00	96.06875	0.40	4.21	$^{12}C_5{}^{1}H_8{}^{14}N_2$
137.10882	551153.11	21.62	137.10787	0.95	6.90	$^{12}C_8{}^{1}H_{13}{}^{14}N_2$

Data:150511_EI_701_Su
Comment:
Description:
Ionization Mode:EI+
History:Average(MS[1] 1.41..1.49)

Acquired:6/12/2015 10:04:40 AM
Operator:AccuTOF
m/z Calibration File:Pos_800-20150601
Created:6/25/2015 10:25:59 AM
Created by:AccuTOF

Charge number:1 Tolerance:2.00[mDa]
Element:^{12}C:0 .. 8, ^{1}H:0 .. 13, ^{11}B:0 .. 0, ^{79}Br:0 .. 0, ^{14}N:0 .. 2, ^{16}O:0 .. 0, ^{32}S:0 .. 1

Unsaturation Number:-1.5 .. 20.0 (Fraction:Both)

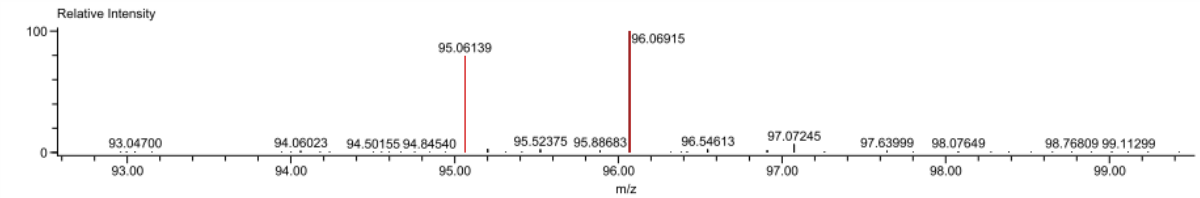

Composition:$C_5H_8N_2$
Mono Isotopic Mass:96.06875 Average Mass:96.13050
Description:

Created:6/25/2015 10:27:37 AM
Nominal Mass:96
Created by:AccuTOF

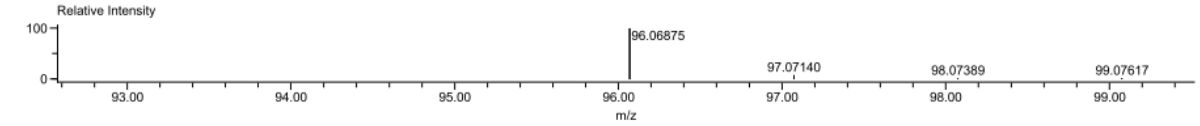

Mass	Intensity	Relative Intensity	Calc. Mass	Mass Difference [mDa]	Mass Difference [ppm]	Possible Formula
33.98769	513486.09	20.14	33.98772	-0.03	-1.00	$^{1}H_2{}^{32}S_1$
95.06139	2017161.45	79.12	95.06092	0.46	4.88	$^{12}C_5{}^{1}H_7{}^{14}N_2$
96.06915	2549640.44	100.00	96.06875	0.40	4.21	$^{12}C_5{}^{1}H_8{}^{14}N_2$
137.10882	551153.11	21.62	137.10787	0.95	6.90	$^{12}C_8{}^{1}H_{13}{}^{14}N_2$

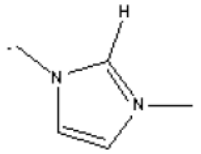

Chemical Formula: $C_5H_8N_2^{\bullet}$
Exact Mass: 96,0687

Data:150511_EI_701_Su
Comment:
Description:
Ionization Mode:EI+
History:Average(MS[1] 1.41..1.49)

Acquired:6/12/2015 10:04:40 AM
Operator:AccuTOF
m/z Calibration File:Pos_800-20150601
Created:6/25/2015 10:25:59 AM
Created by:AccuTOF

Charge number:1 Tolerance:2.00[mDa]
Element:^{12}C:0 .. 8, ^{1}H:0 .. 13, ^{11}B:0 .. 0, ^{79}Br:0 .. 0, ^{14}N:0 .. 2, ^{16}O:0 .. 0, ^{32}S:0 .. 1

Unsaturation Number:-1.5 .. 20.0 (Fraction:Both)

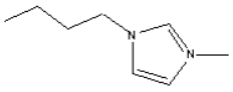

Chemical Formula: $C_8H_{15}N_2$
Exact Mass: 139,1235

Composition:$C_8H_{13}N_2$
Mono Isotopic Mass:137.10787 Average Mass:137.20230
Description:

Created:6/25/2015 10:27:42 AM
Nominal Mass:137
Created by:AccuTOF

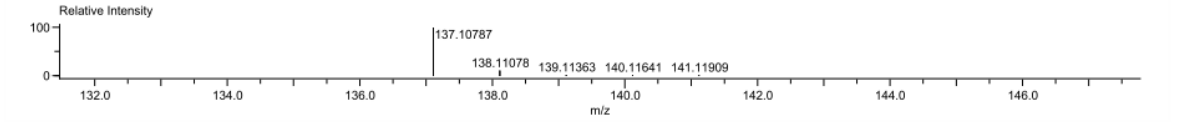

Mass	Intensity	Relative Intensity	Calc. Mass	Mass Difference [mDa]	Mass Difference [ppm]	Possible Formula
33.98769	513486.09	20.14	33.98772	-0.03	-1.00	$^{1}H_2{}^{32}S_1$
95.06139	2017161.45	79.12	95.06092	0.46	4.88	$^{12}C_5{}^{1}H_7{}^{14}N_2$
96.06915	2549640.44	100.00	96.06875	0.40	4.21	$^{12}C_5{}^{1}H_8{}^{14}N_2$
137.10882	551153.11	21.62	137.10787	0.95	6.90	$^{12}C_8{}^{1}H_{13}{}^{14}N_2$

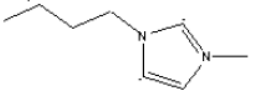

Chemical Formula: $C_8H_{13}N_2^{2+}$
Exact Mass: 137,1079

Data:150511_EI_701_Su
Comment:
Description:
Ionization Mode:EI+
History:Average(MS[1] 0.36..0.39)-1*Average(MS[1] 0.02..0.24),#0-

Acquired:2015-06-12 10:04:40 AM
Operator:AccuTOF
m/z Calibration File:Pos_800-20150601
Created:2015-06-15 1:30:44 PM
Created by:Administrator

Charge number:1 Tolerance:5.00[ppm], 5.00 .. 15.00[mDa] Unsaturation Number:-1.5 .. 20.0 (Fraction:Both)
Element:^{12}C:0 .. 8, ^{1}H:0 .. 14, ^{11}B:0 .. 0, ^{14}N:0 .. 2, ^{16}O:0 .. 2, ^{32}S:0 .. 1

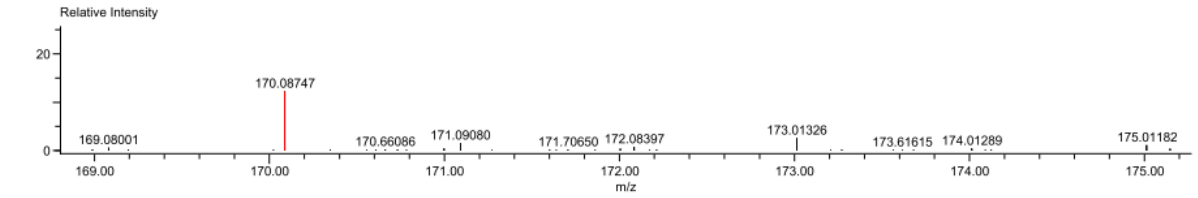

Composition:$C_8H_{14}N_2S$
Mono Isotopic Mass:170.08777 Average Mass:170.27624
Description:

Created:2015-06-15 1:31:22 PM
Nominal Mass:170
Created by:Administrator

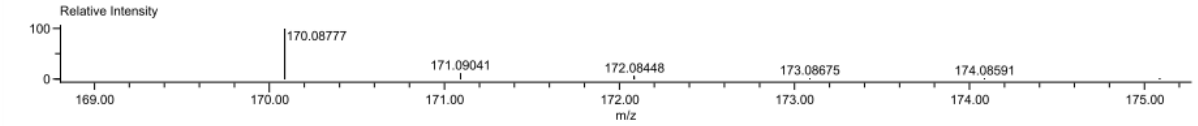

Mass	Intensity	Calc. Mass	Mass Difference [mDa]	Possible Formula
170.08747	111288.84	170.08777	-0.30	$^{12}C_8{}^{1}H_{14}{}^{14}N_2{}^{32}S_1$

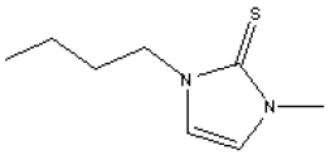

Chemical Formula: $C_8H_{14}N_2S$
Exact Mass: 170,0878

[EMim][HSe], 4

Data:150511_EI_702_Su
Comment:
Description:
Ionization Mode:EI+
History:Average(MS[1] 1.50..1.69)

Acquired:2015-06-12 10:33:26 AM
Operator:AccuTOF
m/z Calibration File:Pos_800-20150601
Created:2015-06-15 1:37:19 PM
Created by:Administrator

Charge number:1 Tolerance:5.00[ppm], 5.00 .. 15.00[mDa] Unsaturation Number:-1.5 .. 20.0 (Fraction:Both)
Element:^{12}C:0 .. 6, ^{1}H:0 .. 12, ^{11}B:0 .. 0, ^{14}N:0 .. 2, ^{16}O:0 .. 0, ^{32}S:0 .. 0, ^{80}Se:0 .. 1

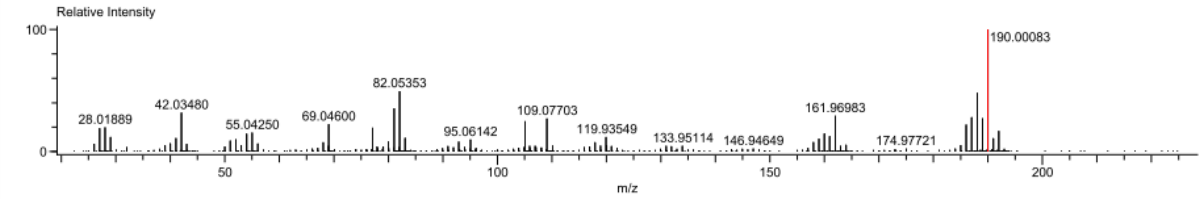

Mass	Intensity	Calc. Mass	Mass Difference [mDa]	Possible Formula
190.00083	219000.43	190.00092	-0.09	$^{12}C_6{}^{1}H_{10}{}^{14}N_2{}^{80}Se_1$

Data:150511_EI_702_Su
Comment:
Description:
Ionization Mode:EI+
History:Average(MS[1] 0.89..0.92)

Acquired:6/12/2015 10:33:26 AM
Operator:AccuTOF
m/z Calibration File:Pos_800-20150601
Created:6/25/2015 10:37:17 AM
Created by:AccuTOF

Charge number:1 Tolerance:2.00[mDa]
Element:^{12}C:0 .. 6, ^{1}H:0 .. 12, ^{11}B:0 .. 0, ^{79}Br:0 .. 0, ^{14}N:0 .. 2, ^{16}O:0 .. 0, ^{32}S:0 .. 0, ^{80}Se:0 .. 1

Unsaturation Number:-1.5 .. 20.0 (Fraction:Both)

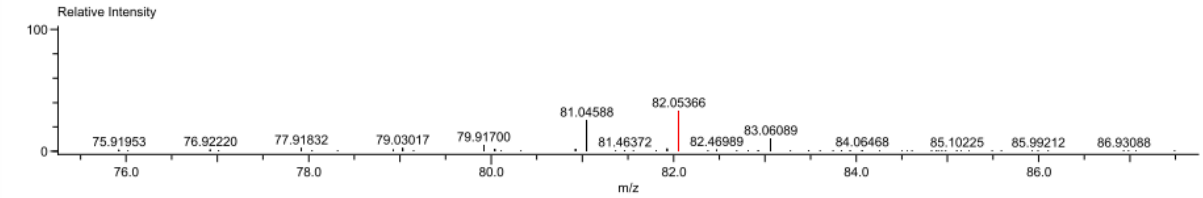

Composition:$C_4H_6N_2$
Mono Isotopic Mass:82.05310 Average Mass:82.10392
Description:

Created:6/25/2015 10:38:40 AM
Nominal Mass:82
Created by:AccuTOF

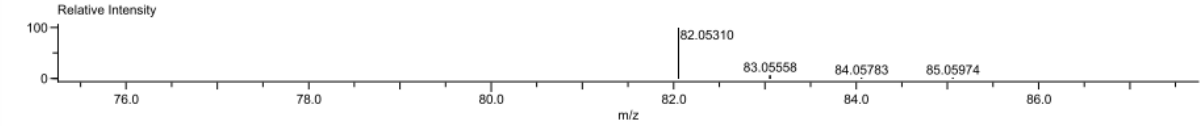

Mass	Intensity	Relative Intensity	Calc. Mass	Mass Difference [mDa]	Mass Difference [ppm]	Possible Formula
82.05366	433457.66	32.62	82.05310	0.56	6.87	$^{12}C_4{}^{1}H_6{}^{14}N_2$
109.07708	265280.75	19.96	109.07657	0.51	4.64	$^{12}C_6{}^{1}H_9{}^{14}N_2$
161.96984	217726.47	16.39	161.96962	0.21	1.33	$^{12}C_4{}^{1}H_6{}^{14}N_2{}^{80}Se_1$
190.00130	1328762.23	100.00	190.00092	0.38	2.01	$^{12}C_6{}^{1}H_{10}{}^{14}N_2{}^{80}Se_1$

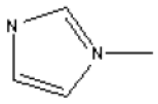

Chemical Formula: $C_4H_6N_2$
Exact Mass: 82,0531

Data:150511_EI_702_Su
Comment:
Description:
Ionization Mode:EI+
History:Average(MS[1] 0.89..0.92)

Acquired:6/12/2015 10:33:26 AM
Operator:AccuTOF
m/z Calibration File:Pos_800-20150601
Created:6/25/2015 10:37:17 AM
Created by:AccuTOF

Charge number:1 Tolerance:2.00[mDa]
Element:^{12}C:0 .. 6, ^{1}H:0 .. 12, ^{11}B:0 .. 0, ^{79}Br:0 .. 0, ^{14}N:0 .. 2, ^{16}O:0 .. 0, ^{32}S:0 .. 0, ^{80}Se:0 .. 1

Unsaturation Number:-1.5 .. 20.0 (Fraction:Both)

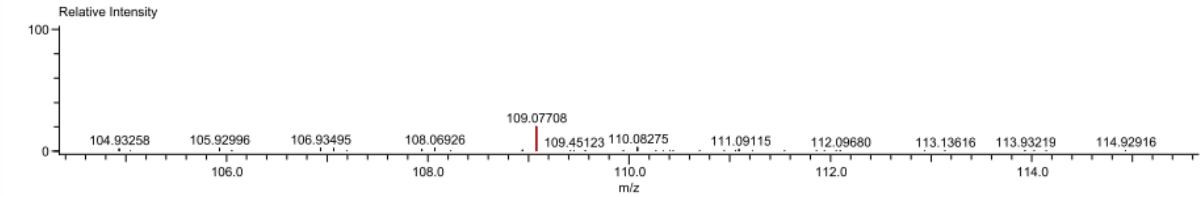

Composition:$C_6H_9N_2$
Mono Isotopic Mass:109.07657 Average Mass:109.14914
Description:

Created:6/25/2015 10:38:57 AM
Nominal Mass:109
Created by:AccuTOF

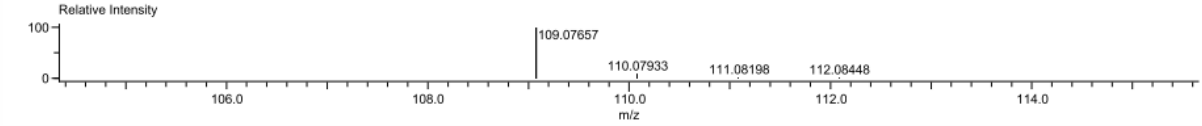

Mass	Intensity	Relative Intensity	Calc. Mass	Mass Difference [mDa]	Mass Difference [ppm]	Possible Formula
82.05366	433457.66	32.62	82.05310	0.56	6.87	$^{12}C_4{}^{1}H_6{}^{14}N_2$
109.07708	265280.75	19.96	109.07657	0.51	4.64	$^{12}C_6{}^{1}H_9{}^{14}N_2$
161.96984	217726.47	16.39	161.96962	0.21	1.33	$^{12}C_4{}^{1}H_6{}^{14}N_2{}^{80}Se_1$
190.00130	1328762.23	100.00	190.00092	0.38	2.01	$^{12}C_6{}^{1}H_{10}{}^{14}N_2{}^{80}Se_1$

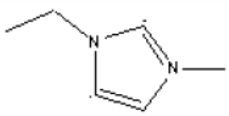

Chemical Formula: $C_6H_9N_2^{2+}$
Exact Mass: 109,0766

Data:150511_EI_702_Su
Comment:
Description:
Ionization Mode:EI+
History:Average(MS[1] 0.89..0.92)

Acquired:6/12/2015 10:33:26 AM
Operator:AccuTOF
m/z Calibration File:Pos_800-20150601
Created:6/25/2015 10:37:17 AM
Created by:AccuTOF

Charge number:1 Tolerance:2.00[mDa]
Element:^{12}C:0 .. 6, ^{1}H:0 .. 12, ^{11}B:0 .. 0, ^{79}Br:0 .. 0, ^{14}N:0 .. 2, ^{16}O:0 .. 0, ^{32}S:0 .. 0, ^{80}Se:0 .. 1

Unsaturation Number:-1.5 .. 20.0 (Fraction:Both)

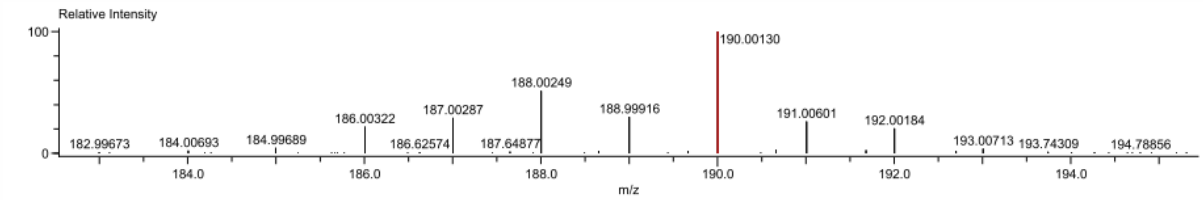

Composition:$C_6H_{10}N_2Se$
Mono Isotopic Mass:190.00092 Average Mass:189.11708
Description:

Created:6/25/2015 10:39:28 AM
Nominal Mass:189
Created by:AccuTOF

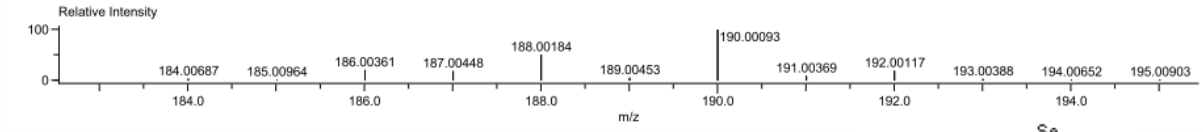

Mass	Intensity	Relative Intensity	Calc. Mass	Mass Difference [mDa]	Mass Difference [ppm]	Possible Formula
82.05366	433457.66	32.62	82.05310	0.56	6.87	$^{12}C_4{}^{1}H_6{}^{14}N_2$
109.07708	265280.75	19.96	109.07657	0.51	4.64	$^{12}C_6{}^{1}H_9{}^{14}N_2$
161.96984	217726.47	16.39	161.96962	0.21	1.33	$^{12}C_4{}^{1}H_6{}^{14}N_2{}^{80}Se_1$
190.00130	1328762.23	100.00	190.00092	0.38	2.01	$^{12}C_6{}^{1}H_{10}{}^{14}N_2{}^{80}Se_1$

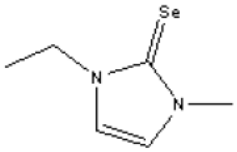

Chemical Formula: $C_6H_{10}N_2Se$
Exact Mass: 190,0009

9. NMR-Spectra

[EMIm][HS], 1

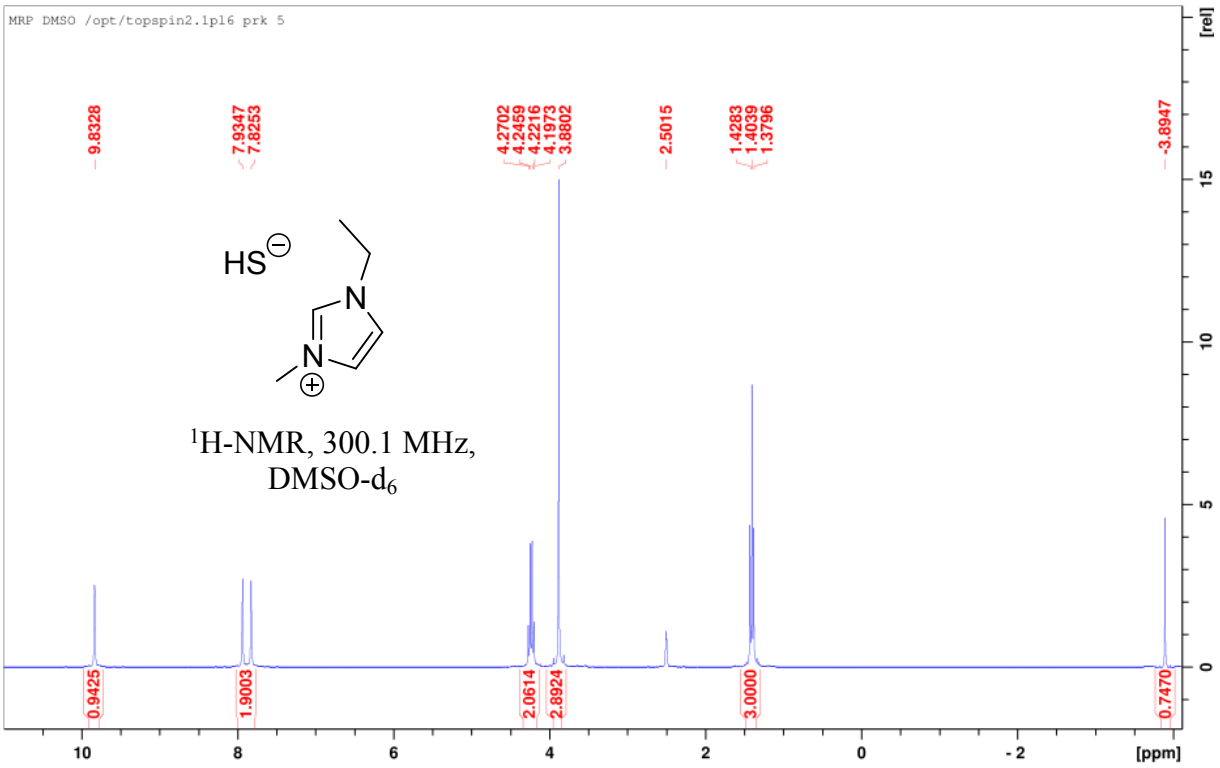

^{1}H-NMR, 300.1 MHz, DMSO-d_6

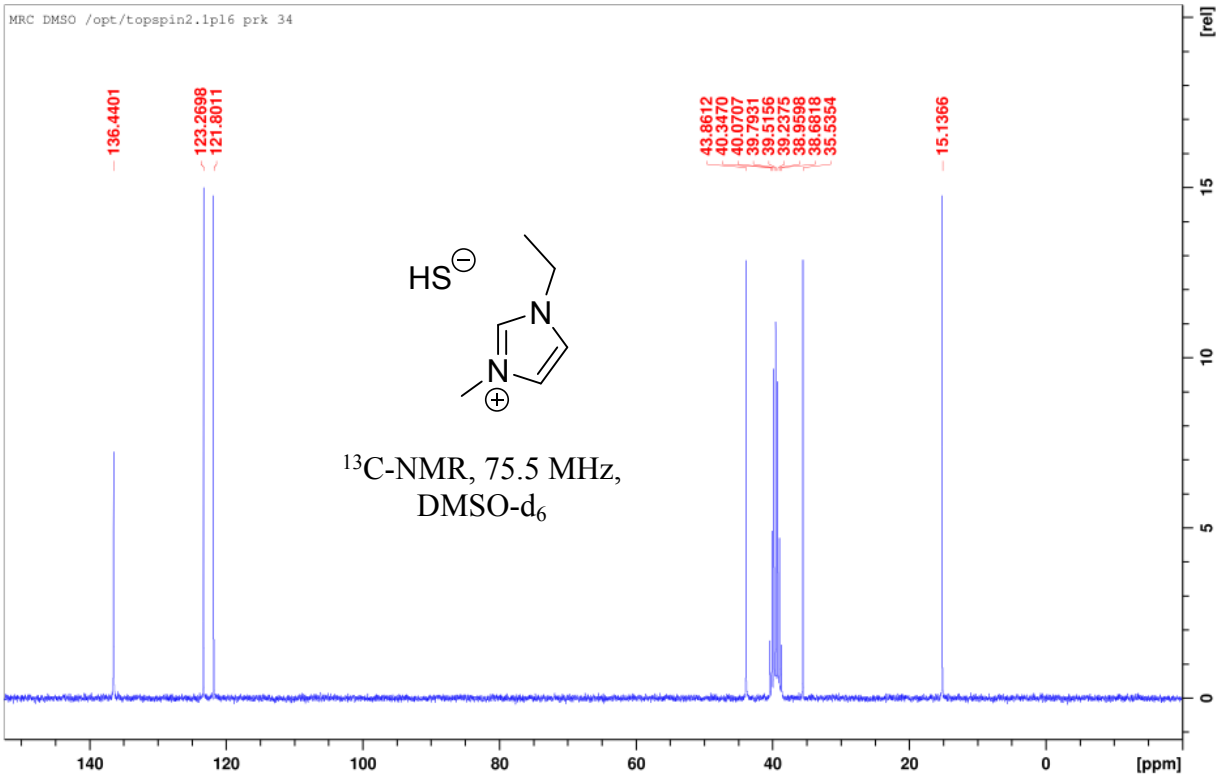

^{13}C-NMR, 75.5 MHz, DMSO-d_6

[EMMIm][HS], 2

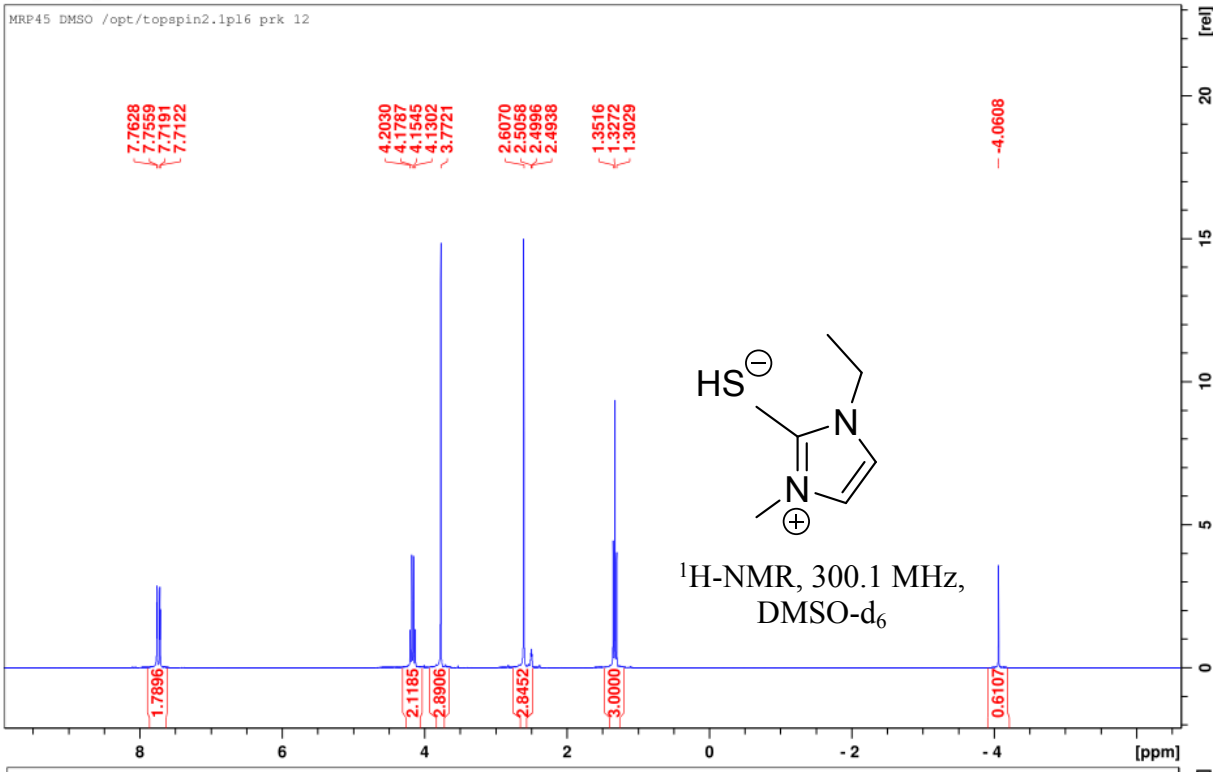
MRP45 DMSO /opt/topspin2.1pl6 prk 12
7.7628
7.7559
7.7191
7.7122
4.2030
4.1787
4.1545
4.1302
3.7721
2.6070
2.5058
2.4996
2.4938
1.3516
1.3272
1.3029
-4.0608
1.7896
2.1185
2.8906
2.8452
3.0000
0.6107
HS
N
N
[1]H-NMR, 300.1 MHz,
DMSO-d6
[rel]
[ppm]

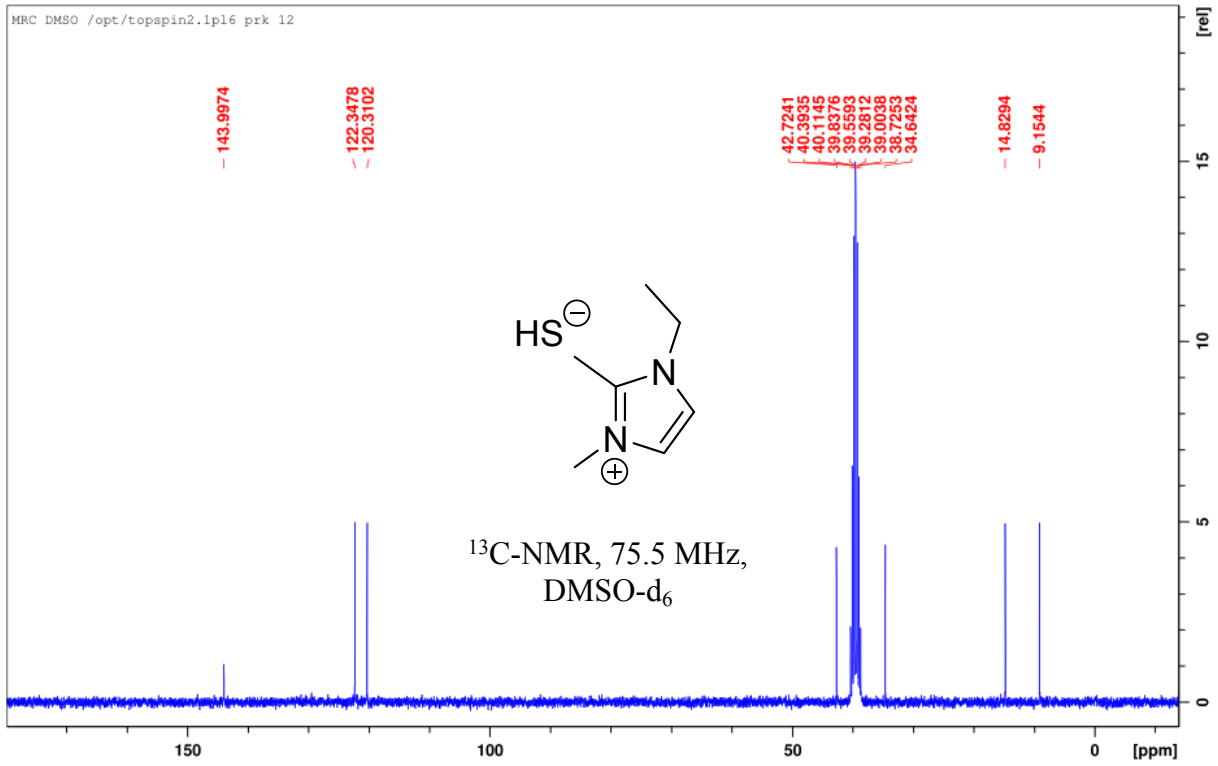
MRC DMSO /opt/topspin2.1pl6 prk 12
143.9974
122.3478
120.3102
42.7241
40.3935
40.1145
39.8376
39.5593
39.2812
39.0038
38.7253
34.6424
14.8294
9.1544
HS
N
N
[13]C-NMR, 75.5 MHz,
DMSO-d6
[rel]
[ppm]

[BMIm][HS], 3

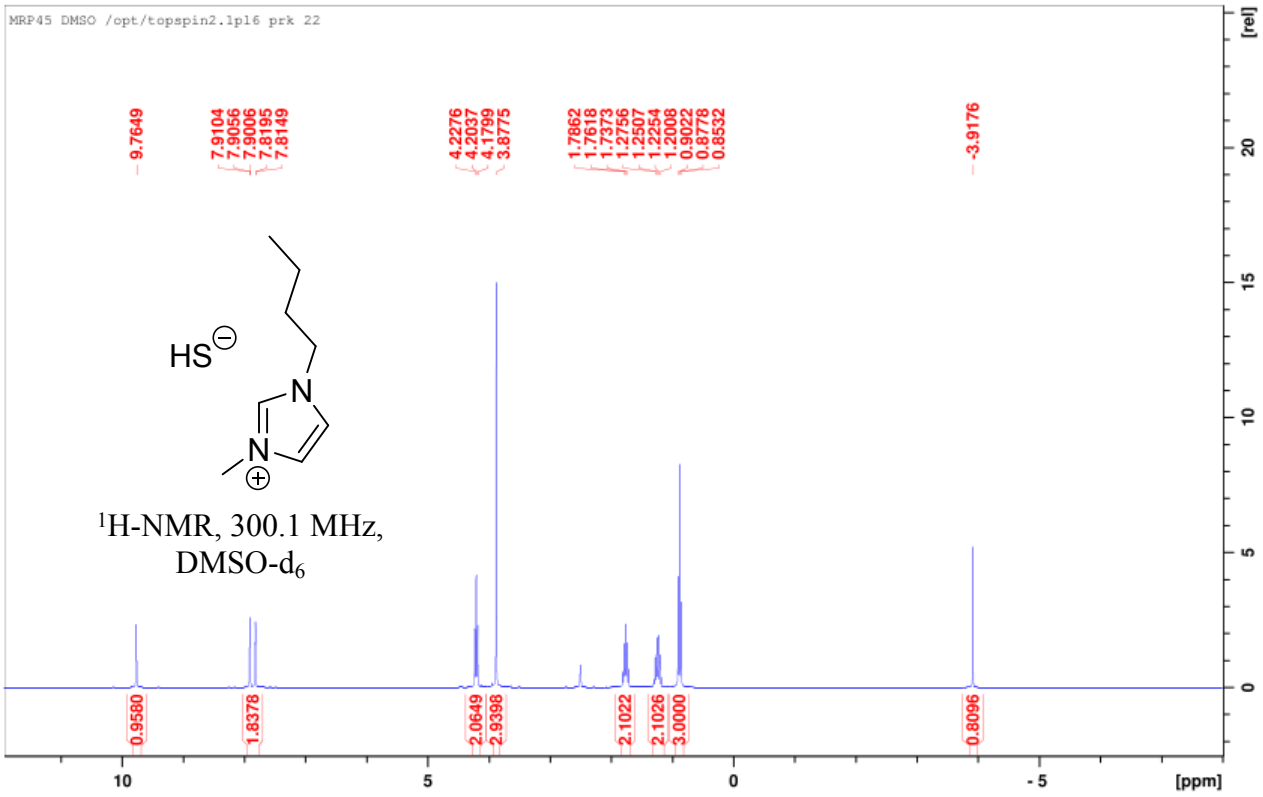
MRP45 DMSO /opt/topspin2.lp16 prk 22
9.7649
7.9104
7.9056
7.9006
7.8195
7.8149
4.2276
4.2037
4.1799
3.8775
1.7862
1.7618
1.7373
1.2756
1.2507
1.2254
1.2008
0.9022
0.8778
0.8532
-3.9176
HS⊖
N
N⊕
^{1}H-NMR, 300.1 MHz,
DMSO-d$_6$
0.9580
1.8378
2.0649
2.9398
2.1022
2.1026
3.0000
0.8096
10
5
0
- 5
[ppm]
[rel]

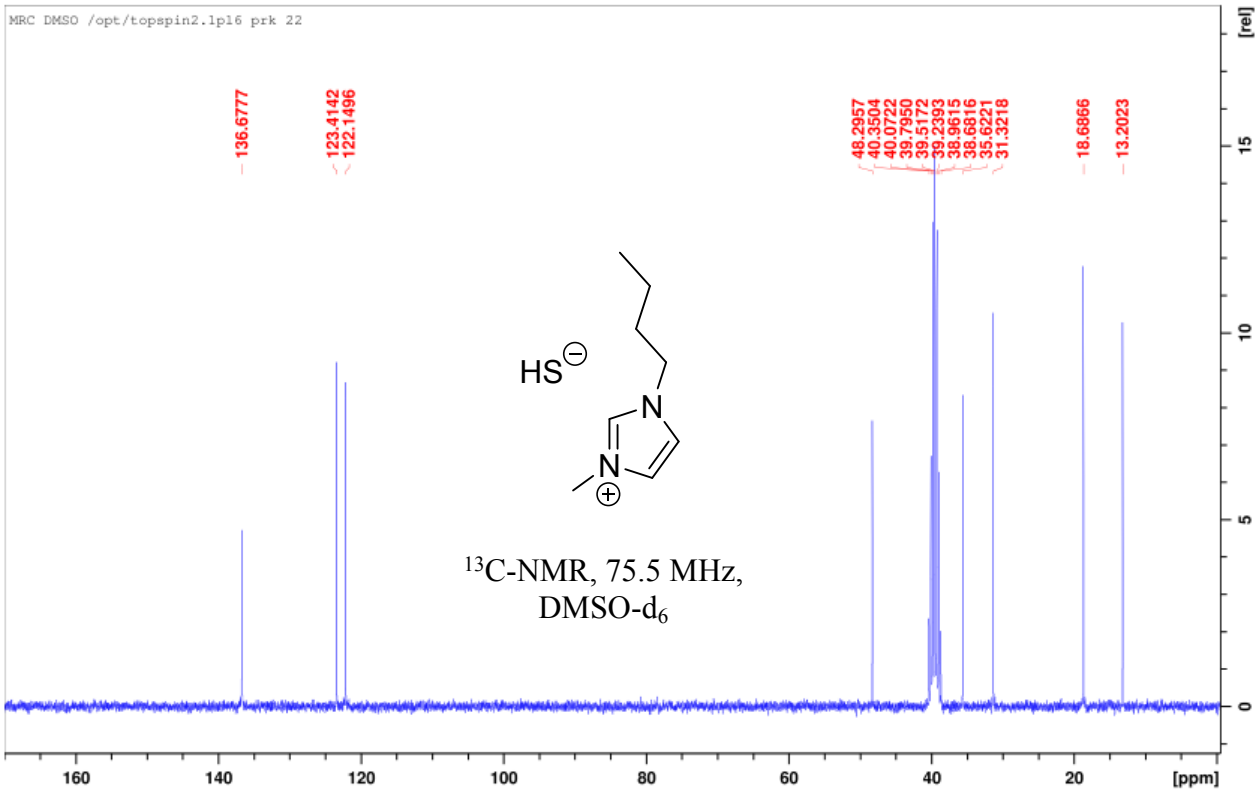
MRC DMSO /opt/topspin2.lp16 prk 22
136.6777
123.4142
122.1496
48.2957
40.3504
40.0722
39.7950
39.5172
39.2393
38.9615
38.6816
35.6221
31.3218
18.6866
13.2023
HS⊖
N
N⊕
^{13}C-NMR, 75.5 MHz,
DMSO-d$_6$
160
140
120
100
80
60
40
20
[ppm]
[rel]

[EMIm][HSe], 4

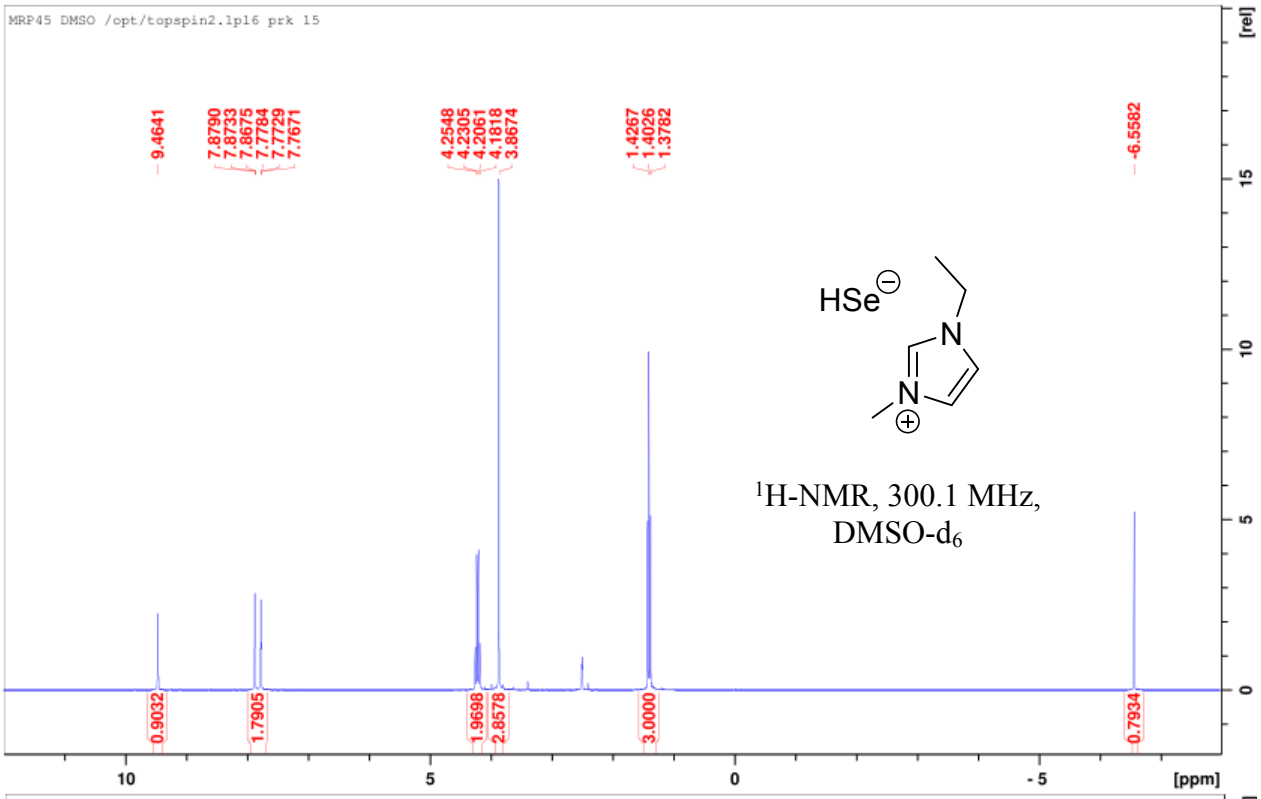
MRP45 DMSO /opt/topspin2.1p16 prk 15
9.4641
7.8790
7.8733
7.8675
7.7784
7.7729
7.7671
4.2548
4.2305
4.2061
4.1818
3.8674
1.4267
1.4026
1.3782
-6.5582
0.9032
1.7905
1.9698
2.8578
3.0000
0.7934
HSe
N
N
[1]H-NMR, 300.1 MHz,
DMSO-d6
10
5
0
-5
[ppm]
[rel]

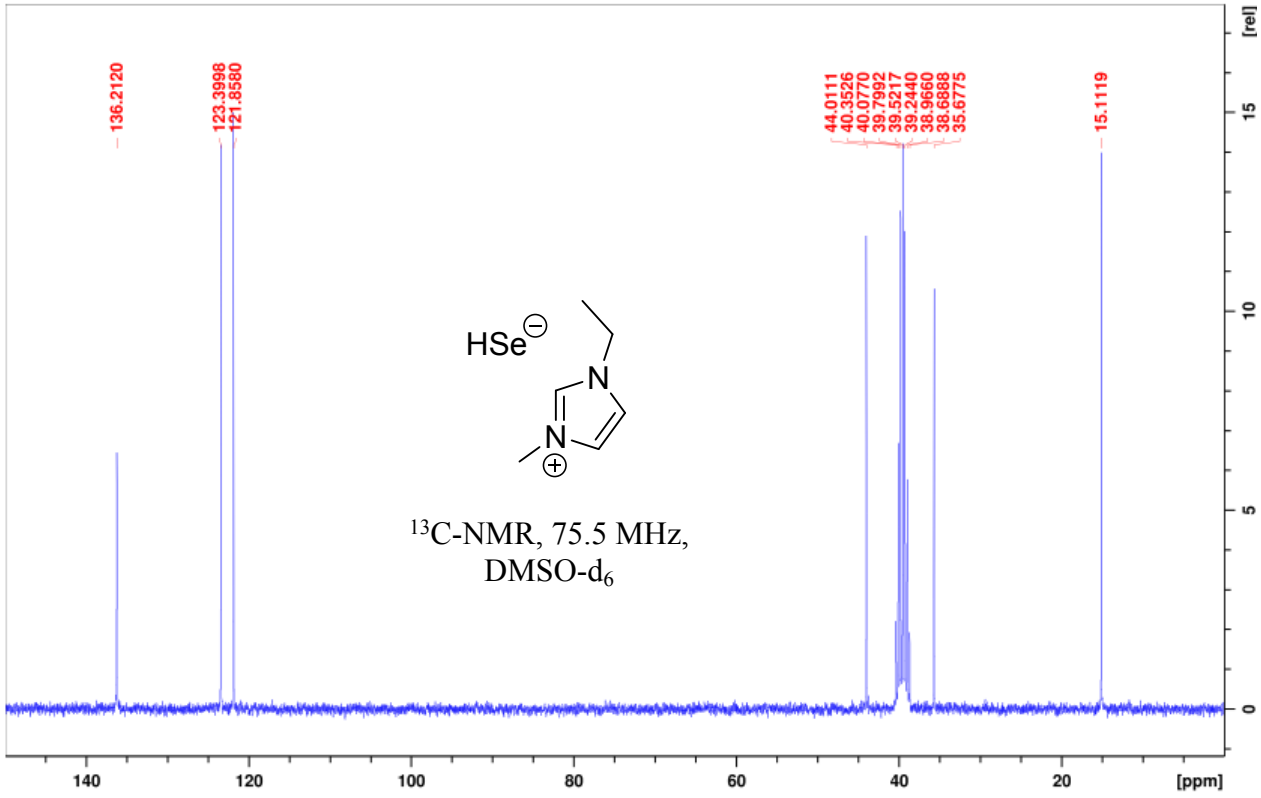
136.2120
123.3998
121.8580
44.0111
40.3526
40.0770
39.7992
39.5217
39.2440
38.9660
38.6888
35.6775
15.1119
HSe
N
N
[13]C-NMR, 75.5 MHz,
DMSO-d6
140
120
100
80
60
40
20
[ppm]
[rel]

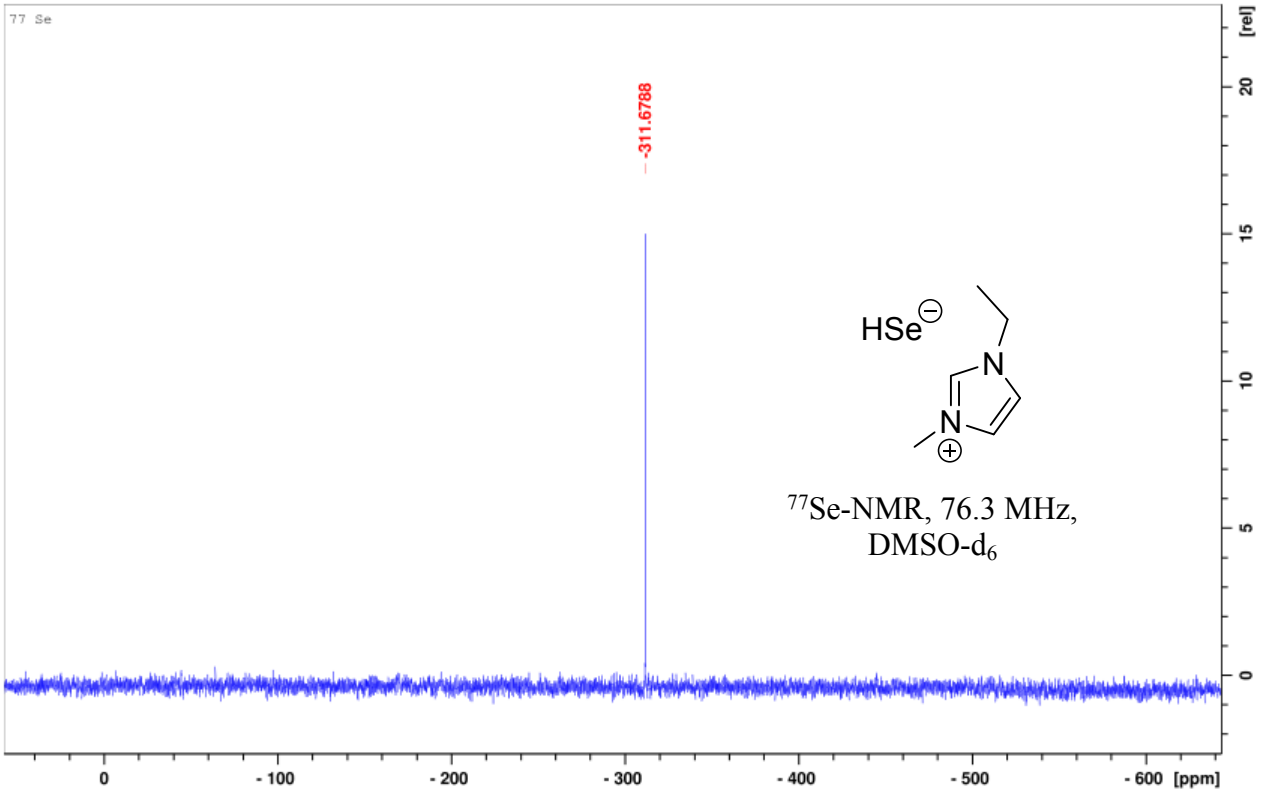

^{77}Se-NMR, 76.3 MHz,
DMSO-d$_6$

[BMPyr][HS], 5

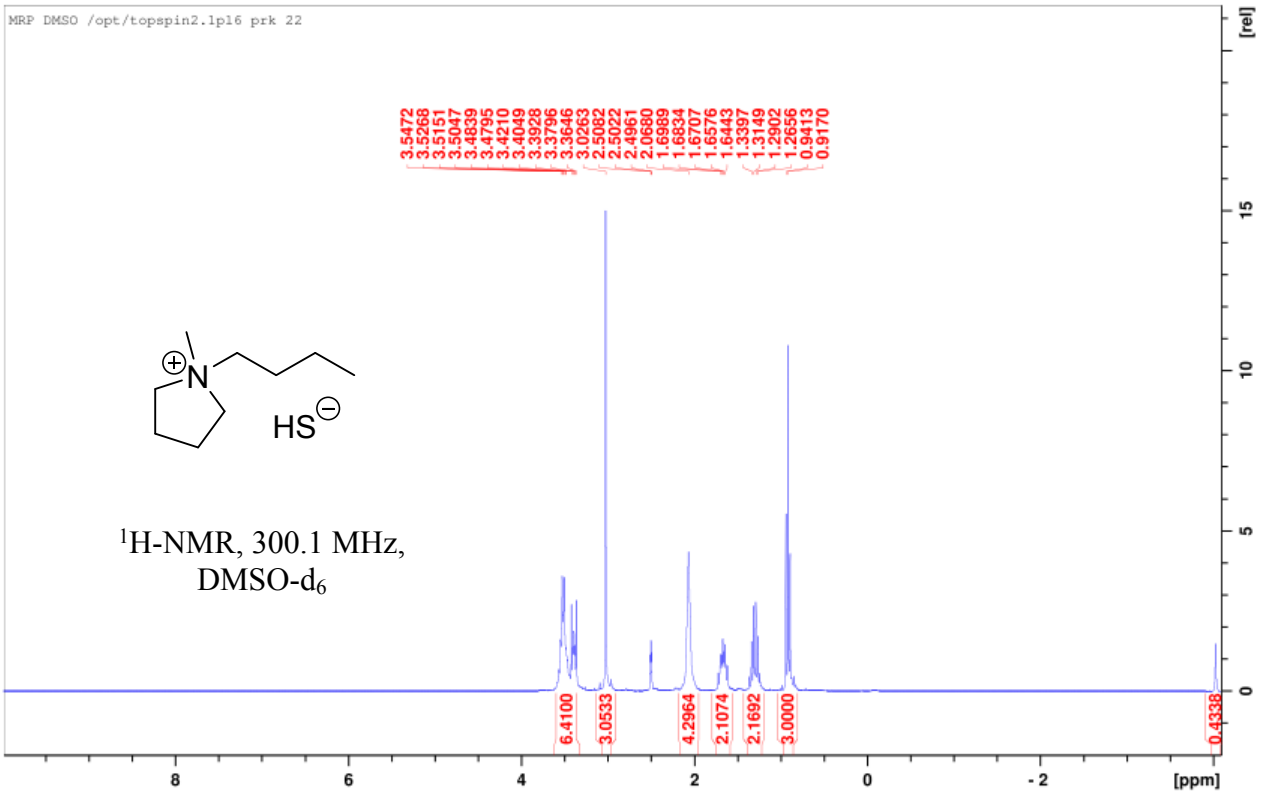

^{1}H-NMR, 300.1 MHz,
DMSO-d$_6$

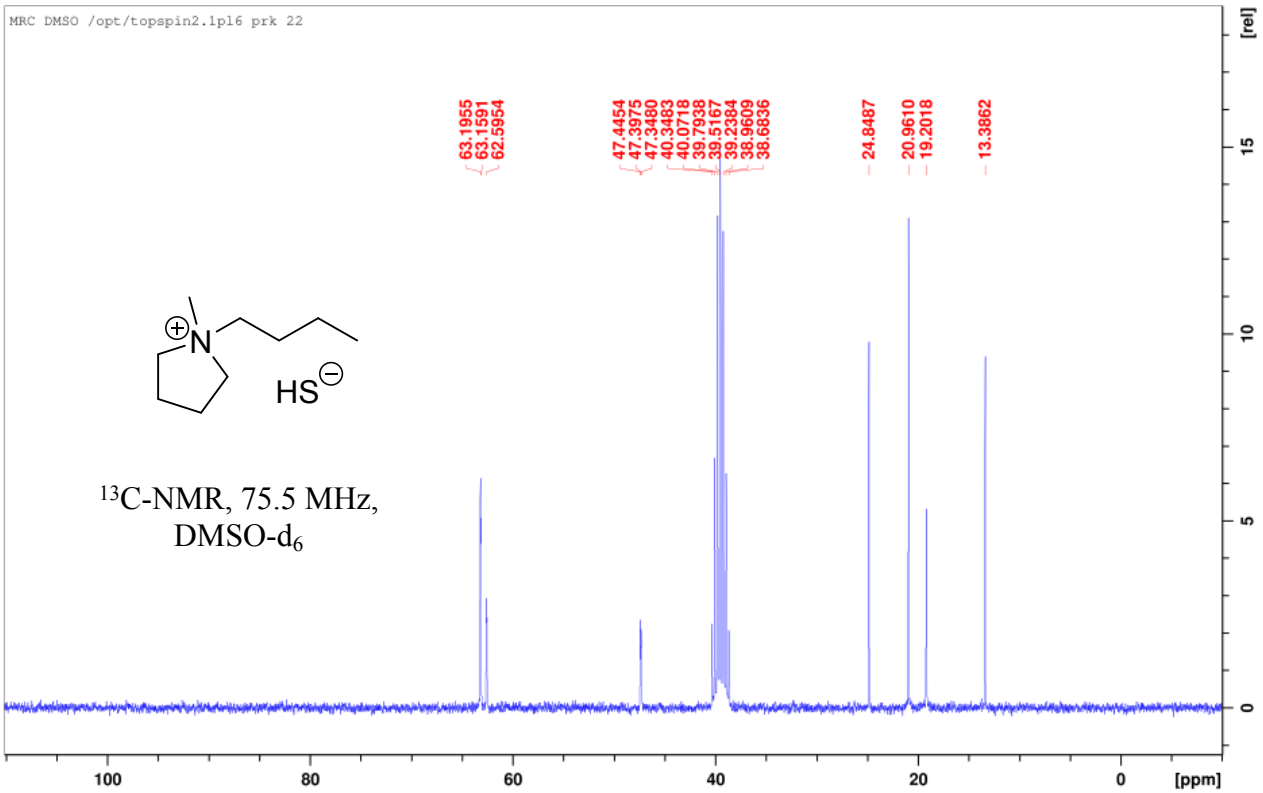

10. IR-Spectra

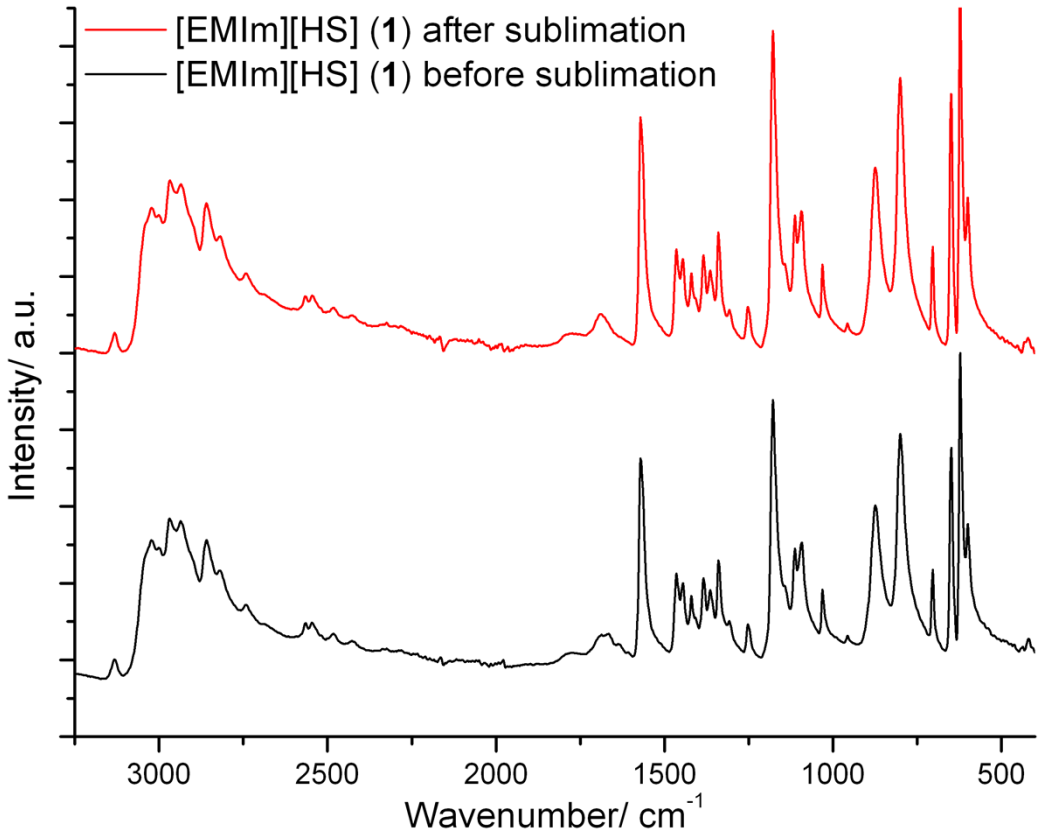

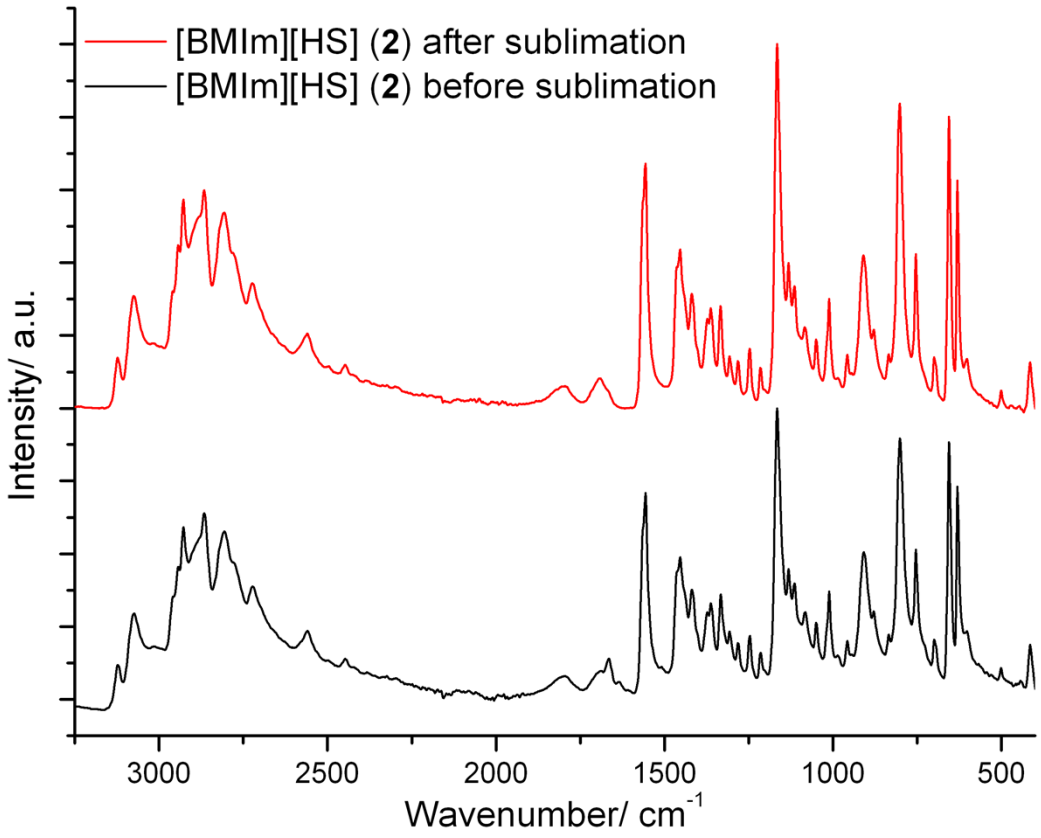
[BMIm][HS] (2) after sublimation
[BMIm][HS] (2) before sublimation
Intensity/ a.u.
3000
2500
2000
1500
1000
500
Wavenumber/ cm-1

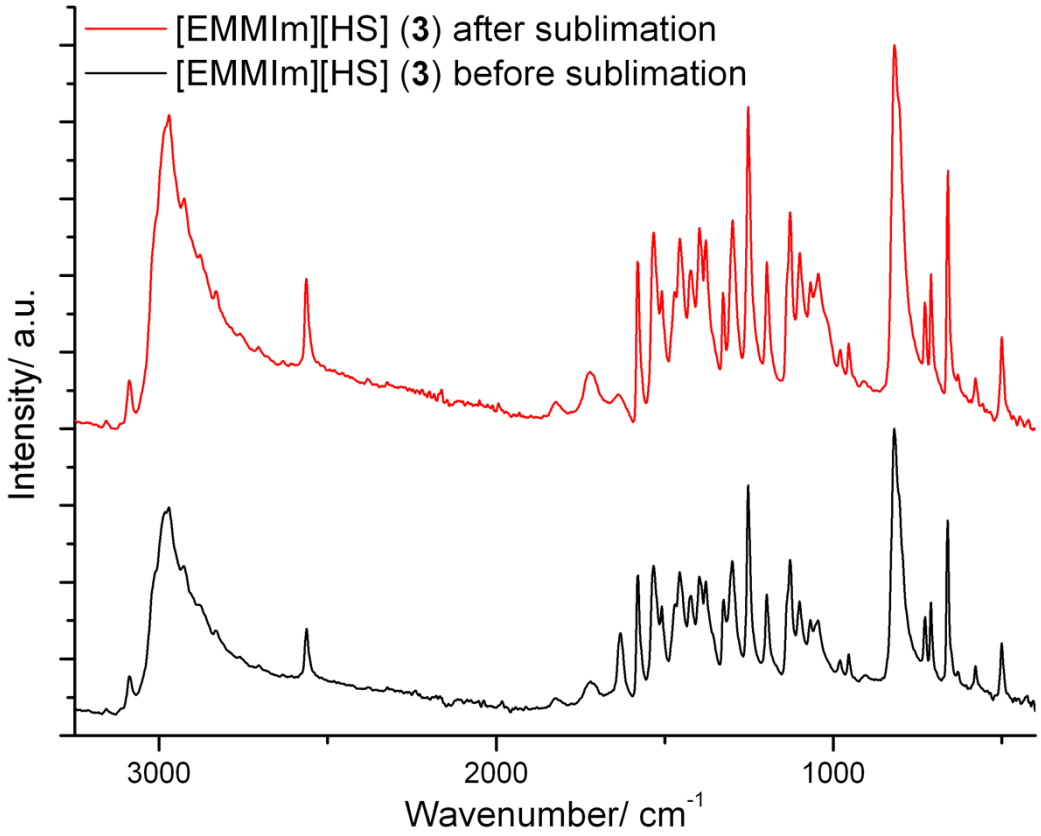
[EMMIm][HS] (3) after sublimation
[EMMIm][HS] (3) before sublimation
Intensity/ a.u.
3000
2000
1000
Wavenumber/ cm-1

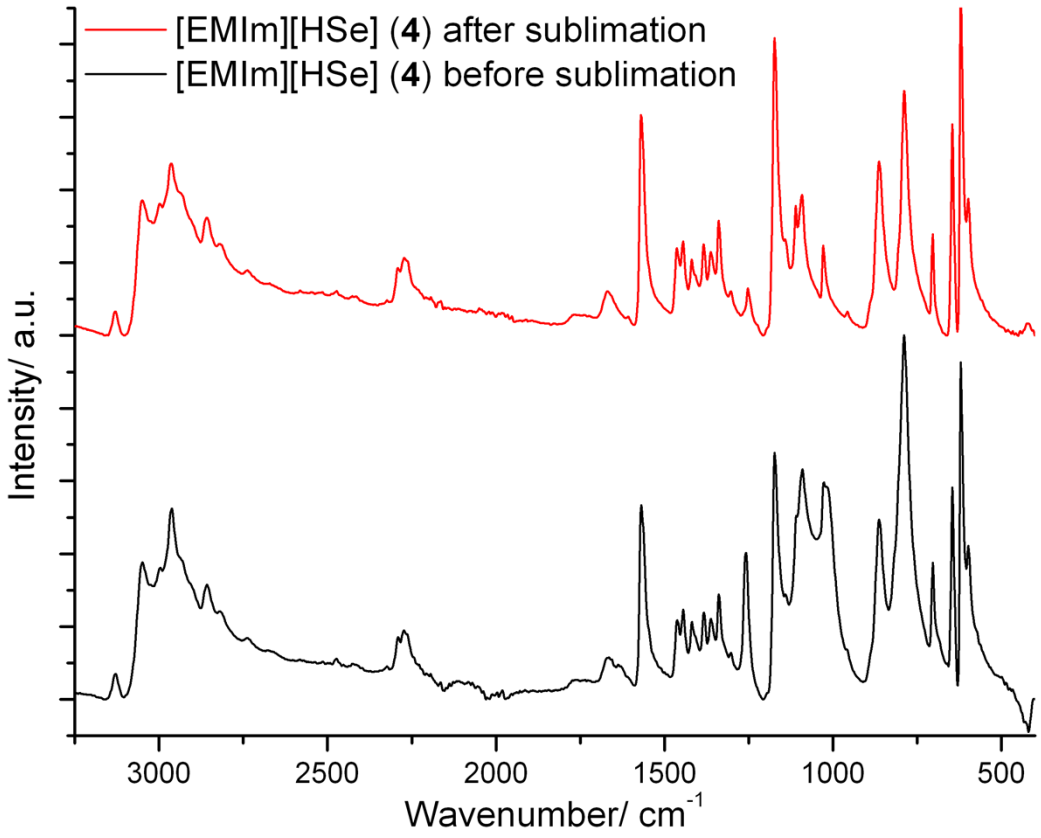
[EMIm][HSe] (4) after sublimation
[EMIm][HSe] (4) before sublimation
Intensity/ a.u.
3000
2500
2000
1500
1000
500
Wavenumber/ cm-1

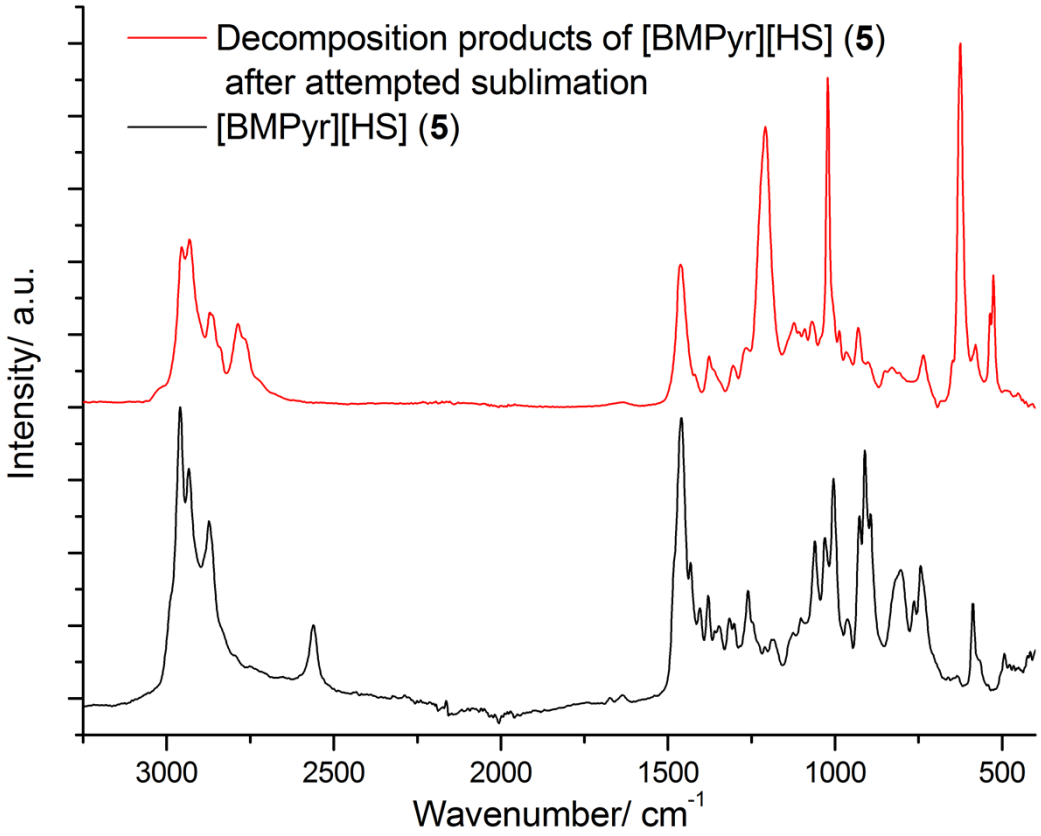
Decomposition products of [BMPyr][HS] (5)
after attempted sublimation
[BMPyr][HS] (5)
Intensity/ a.u.
3000
2500
2000
1500
1000
500
Wavenumber/ cm-1

11. References

1 G. R. Fulmer, A. J. M. Miller, H. E. Gottlieb, N. H. Sherden, A. Nudelman, B. M. Stoltz, K. I. Goldberg and J. E. Bercaw, *Organometallics*, 2010, **29**, 2176.

2 W. L. Amarego and D. D. Perrin, *Purification of Laboratory Chemicals*, Elsevier, Burlington, 1996.

3 J. E. Bara, *Ind. Eng. Chem. Res.*, 2011, **50**, 13614.

4(a) R. Kalb (PROIONIC), WO 2008 052 861, **2008**; (b) (PROIONIC), WO 2008 052 860, **2008**.

5(a) J.-H. So and P. Boudjouk, *Synthesis*, 1989, 306; (b) M. W. DeGroot, N. J. Taylor and J. F. Corrigan, *J. Mater. Chem.*, 2004, **14**, 654.

6 Bruker Instrument Service v3.0.26, APEX2 v2012.10-0, SAINT v8.27B, Bruker, Bruker AXS Inc., Madison, Wisconsin, USA, 2012.

7 A. Altomare, M. C. Burla, M. Camalli, G. Cascarano, C. Giacovazzo, A. Guagliardi, A. G. G. Moliterni, G. Polidori and R. Spagna, *J. Appl. Crystallogr.*, 1999, **32**, 115.

8 M. C. Burla, R. Caliandro, M. Camalli, B. Carrozzini, G. L. Cascarano, C. Giacovazzo, M. Mallamo, A. Mazzone, G. Polidori and R. Spagna, *J. Appl. Cryst.*, 2012, **45**, 357.

9 G. Sheldrick, *Acta Cryst. A*, 2008, **64**, 112.

10 A. L. Spek, *Acta Cryst. D*, 2009, **65**, 148.

11 L. Farrugia, *J. Appl. Cryst.*, 2012, **45**, 849.

12 F. H. Allen, O. Johnson, G. P. Shields, B. R. Smith and M. Towler, *J. Appl. Crystallogr.*, 2004, **37**, 335.

13 SADABS v2012/1, Bruker, Bruker AXS Inc., Madison, Wisconsin, USA, 2012.

14 Diamond - Crystal and Molecular Structure Visualization v3.2i, K. Brandenburg and H. Putz, Crystal Impact GbR, Bonn, Germany, 2012.

15 G. Illuminati and C. Lillocci, *J. Org. Chem.*, 1977, **42**, 2201.

16(a) D. M. Price, *Thermochim. Acta*, 2001, **367–368**, 253; (b) W. E. Acree, Jr. and J. S. Chickos, in *NIST Chemistry WebBook, NIST Standard Reference Database Number 69*, eds. P. J. Linstrom and W. G. Mallard, National Institute of Standards and Technology, Gaithersburg MD, 20899, http://webbook.nist.gov, (retrieved June 26, 2015).

17 S. P. Verevkin, D. H. Zaitsau, V. N. Emelyanenko, A. V. Yermalayeu, C. Schick, H. Liu, E. J. Maginn, S. Bulut, I. Krossing and R. Kalb, *J. Phys. Chem. B*, 2013, **117**, 6473.

18 Gaussian 09, Revision C.01, M. J. Frisch, G. W. Trucks, H. B. Schlegel, G. E. Scuseria, M. A. Robb, J. R. Cheeseman, G. Scalmani, V. Barone, B. Mennucci, G. A. Petersson, H. Nakatsuji, M. Caricato, X. Li, H. P. Hratchian, A. F. Izmaylov, J. Bloino, G. Zheng, J. L. Sonnenberg, M. Hada, M. Ehara, K. Toyota, R. Fukuda, J. Hasegawa, M. Ishida, T. Nakajima, Y. Honda, O. Kitao, H. Nakai, T. Vreven, J. A. Montgomery Jr., J. E. Peralta, F. Ogliaro, M. J. Bearpark, J. Heyd, E. N. Brothers, K. N. Kudin, V. N. Staroverov, R. Kobayashi, J. Normand, K. Raghavachari, A. P. Rendell, J. C. Burant, S. S. Iyengar, J. Tomasi, M. Cossi, N. Rega, N. J. Millam, M. Klene, J. E. Knox, J. B. Cross, V. Bakken, C. Adamo, J. Jaramillo, R. Gomperts, R. E. Stratmann, O. Yazyev, A. J. Austin, R. Cammi, C. Pomelli, J. W. Ochterski, R. L. Martin, K. Morokuma, V. G. Zakrzewski, G. A. Voth, P. Salvador, J. J. Dannenberg, S. Dapprich, A. D. Daniels, Ö. Farkas, J. B. Foresman, J. V. Ortiz, J. Cioslowski and D. J. Fox, Gaussian, Inc., Wallingford, CT, USA, 2010.

19(a) J. P. Perdew, *Phys. Rev. B*, 1986, **33**, 8822; (b) A. D. Becke, *Phys. Rev. A*, 1988, **38**, 3098; (c) F. Weigend and R. Ahlrichs, *Phys. Chem. Chem. Phys.*, 2005, **7**, 3297; (d) F. Weigend, *Phys. Chem. Chem. Phys.*, 2006, **8**, 1057.

20 AIMAll (Version 14.11.23), T. A. Keith, TK Gristmill Software, Overland Park KS, USA, 2014.
21 R. F. W. Bader, *J. Phys. Chem. A*, 2009, **113**, 10391.
22(a) F. Jensen, *Introduction to Computational Chemistry*, John Wiley & Sons Ltd, Chichester, 2007; (b) A. E. Reed, L. A. Curtiss and F. Weinhold, *Chem. Rev.*, 1988, **88**, 899.
23 NBO Version 3.1, E. D. Glendening, A. E. Reed, J. E. Carpenter and F. Weinhold, Theoretical Chemistry Institute, University of Wisconsin, Madison.
24 M. v. Hopffgarten and G. Frenking, *Wiley Interdiscip. Rev.: Comput. Mol. Sci.*, 2012, **2**, 43.
25(a) C. Fonseca Guerra, J. G. Snijders, G. te Velde and E. J. Baerends, *Theor. Chem. Acc.*, 1998, **99**, 391; (b) G. te Velde, F. M. Bickelhaupt, E. J. Baerends, C. Fonseca Guerra, S. J. A. van Gisbergen, J. G. Snijders and T. Ziegler, *J. Comput. Chem.*, 2001, **22**, 931; (c) ADF2014, SCM, E. J. Baerends, T. Ziegler, J. Autschbach, D. Bashford, A. Bérces, F. M. Bickelhaupt, C. Bo, P. M. Boerrigter, L. Cavallo, D. P. Chong, L. Deng, R. M. Dickson, D. E. Ellis, M. v. Faassen, L. Fan, T. H. Fischer, C. F. Guerra, M. Franchini, A. Ghysels, A. Giammona, S. J. A. v. Gisbergen, A. W. Götz, J. A. Groeneveld, O. V. Gritsenko, M. Grüning, S. Gusarov, F. E. Harris, P. v. d. Hoek, C. R. Jacob, H. Jacobsen, L. Jensen, J. W. Kaminski, G. v. Kessel, F. Kootstra, A. Kovalenko, M. V. Krykunov, E. v. Lenthe, D. A. McCormack, A. Michalak, M. Mitoraj, S. M. Morton, J. Neugebauer, V. P. Nicu, L. Noodleman, V. P. Osinga, S. Patchkovskii, M. Pavanello, P. H. T. Philipsen, D. Post, C. C. Pye, W. Ravenek, J. I. Rodríguez, P. Ros, P. R. T. Schipper, H. v. Schoot, G. Schreckenbach, J. S. Seldenthuis, M. Seth, J. G. Snijders, M. Solà, M. Swart, D. Swerhone, G. t. Velde, P. Vernooijs, L. Versluis, L. Visscher, O. Visser, F. Wang, T. A. Wesolowski, E. M. v. Wezenbeek, G. Wiesenekker, S. K. Wolff, T. K. Woo and A. L. Yakovlev, Theoretical Chemistry, Vrije Universiteit, Amsterdam, The Netherlands, http://www.scm.com.
26 J. P. Perdew, K. Burke and M. Ernzerhof, *Phys. Rev. Lett.*, 1996, **77**, 3865.
27 G. Kresse and D. Joubert, *Phys. Rev. B*, 1999, **59**, 1758.
28 G. Kresse and J. Furthmüller, *Phys. Rev. B*, 1996, **54**, 11169.
29 S. Grimme, J. Antony, S. Ehrlich and H. Krieg, *J. Chem. Phys.*, 2010, **132**, 154104.
30 O. Holloczki, D. Gerhard, K. Massone, L. Szarvas, B. Nemeth, T. Veszpremi and L. Nyulaszi, *New J. Chem.*, 2010, **34**, 3004.
31(a) A. J. Ellis and R. M. Golding, *J. Chem. Soc.*, 1959, 127; (b) E. M. Higgins, J. A. Sherwood, A. G. Lindsay, J. Armstrong, R. S. Massey, R. W. Alder and A. C. O'Donoghue, *Chem. Commun.*, 2011, **47**, 1559.
32 C. F. Matta and R. J. Boyd, in *The Quantum Theory of Atoms in Molecules*, eds. C. F. Matta and R. J. Boyd, Wiley-VCH, Weinheim, 2007, pp. 1-34.